US Army Corps
of Engineers
Construction Engineering
Research Laboratories

USACERL Technical Report 98/60
April 1998

Pyrolysis/Gas Chromatography/Mass Spectrometry of Energetic Materials

by
Donald M. Cropek
Patricia A. Kemme
Jean M. Day

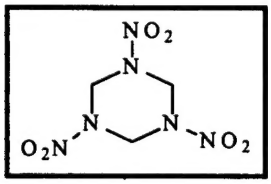

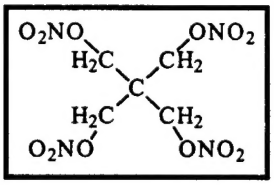

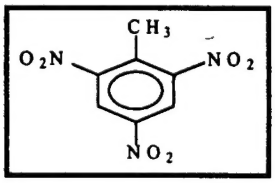

The armaments industry generates approximately 1600 tons per year of hazardous waste containing explosives and propellants. By far, the most common disposal method for this hazardous waste is open burning/open detonation (OB/OD). Unfortunately, OB/OD has the potential to create environmental problems due to uncontrolled emission of by-products. Incineration is currently the most mature and well-characterized alternative disposal technology. In the event that OB/OD is curtailed or even eliminated, studies examining incineration as a back-up treatment technology could have an immediate impact on mission readiness, especially if the focus of the work is on characterization and reduction of emissions. The objective of this work was to examine the pyrolysis of energetic materials and to study the by-products produced during thermal decomposition in the absence of oxygen. Pyrolytic by-products from RDX, TNT, and PETN were examined. Samples were prepared and analyzed, results were studied and compared with work done in previous studies, and recommendations for further research were made.

USER EVALUATION OF REPORT

REFERENCE: USACERL Technical Report 98/60, *Pyrolysis/Gas Chromatography/Mass Spectrometry of Energetic Materials*

Please take a few minutes to answer the questions below, tear out this sheet, and return it to USACERL. As user of this report, your customer comments will provide USACERL with information essential for improving future reports.

1. Does this report satisfy a need? (Comment on purpose, related project, or other area of interest for which report will be used.)

_____

_____

_____

2. How, specifically, is the report being used? (Information source, design data or procedure, management procedure, source of ideas, etc.)

_____

_____

3. Has the information in this report led to any quantitative savings as far as manhours/contract dollars saved, operating costs avoided, efficiencies achieved, etc.? If so, please elaborate.

_____

_____

4. What is your evaluation of this report in the following areas?

   a. Presentation: _____

   b. Completeness: _____

   c. Easy to Understand: _____

   d. Easy to Implement: _____

   e. Adequate Reference Material: _____

   f. Relates to Area of Interest: _____

   g. Did the report meet your expectations? _____

   h. Does the report raise unanswered questions? _____

i. General Comments. (Indicate what you think should be changed to make this report and future reports of this type more responsive to your needs, more usable, improve readability, etc.)

_____

_____

_____

_____

_____

_____

5. If you would like to be contacted by the personnel who prepared this report to raise specific questions or discuss the topic, please fill in the following information.

Name: _____

Telephone Number: _____

Organization Address: _____

_____

_____

6. Please mail the completed form to:

Department of the Army
CONSTRUCTION ENGINEERING RESEARCH LABORATORIES
ATTN: CECER-TR-I
P.O. Box 9005
Champaign, IL 61826-9005

REPORT DOCUMENTATION PAGE

Form Approved
OMB No. 0704-0188

1. AGENCY USE ONLY *(Leave Blank)*	2. REPORT DATE	3. REPORT TYPE AND DATES COVERED
	April 1998	Final

4. TITLE AND SUBTITLE
Pyrolysis/Gas Chromatography/Mass Spectrometry of Energetic Materials

5. FUNDING NUMBERS
4A162720
D048
EP-UC5

6. AUTHOR(S)
Donald M. Cropek, Patricia A. Kemme, and Jean M. Day

7. PERFORMING ORGANIZATION NAME(S) AND ADDRESS(ES)
U.S. Army Construction Engineering Research Laboratories (USACERL)
P.O. Box 9005
Champaign, IL 61826-9005

8. PERFORMING ORGANIZATION REPORT NUMBER
TR 98/60

9. SPONSORING / MONITORING AGENCY NAME(S) AND ADDRESS(ES)
Headquarters, U.S. Army Environmental Center (USAEC)
ATTN: SFIM-AEC-TS
PO Box 4435
Aberdeen Proving Ground, MD 21010-5401

10. SPONSORING / MONITORING AGENCY REPORT NUMBER

11. SUPPLEMENTARY NOTES
Copies are available from the National Technical Information Service, 5285 Port Royal Road, Springfield, VA 22161.

12a. DISTRIBUTION / AVAILABILITY STATEMENT
Approved for public release; distribution is unlimited.

12b. DISTRIBUTION CODE

13. ABSTRACT (Maximum 200 words)
The armaments industry generates approximately 1600 tons per year of hazardous waste containing explosives and propellants. By far, the most common disposal method for this hazardous waste is open burning/open detonation (OB/OD). Unfortunately, OB/OD has the potential to create environmental problems due to uncontrolled emission of by-products. Incineration is currently the most mature and well-characterized alternative disposal technology. In the event that OB/OD is curtailed or even eliminated, studies examining incineration as a back-up treatment technology could have an immediate impact on mission readiness, especially if the focus of the work is on characterization and reduction of emissions. The objective of this work was to examine the pyrolysis of energetic materials and to study the by-products produced during thermal decomposition in the absence of oxygen. Pyrolytic by-products from RDX, TNT, and PETN were examined. Samples were prepared and analyzed, results were studied and compared with work done in previous studies, and recommendations for further research were made.

14. SUBJECT TERMS
pyrolysis
munitions waste disposal
hazardous waste management
energetic material (EM) waste

15. NUMBER OF PAGES
66

16. PRICE CODE

17. SECURITY CLASSIFICATION OF REPORT	18. SECURITY CLASSIFICATION OF THIS PAGE	19. SECURITY CLASSIFICATION OF ABSTRACT	20. LIMITATION OF ABSTRACT
Unclassified	Unclassified	Unclassified	SAR

Foreword

This study was conducted for Headquarters, U.S. Army Corps of Engineers under Project 4A162720D048, "Industrial Operations Pollution Control Technology"; Work Unit EP-UC5, "Studies of Pyrolytic Behavior of Energetic Materials." The technical monitor was R. Eichholtz, SFIM-AEC-TS.

The work was performed by the Industrial Operations Division (UL-I) of the Utilities and Industrial Operations Laboratory (UL), U.S. Army Construction Engineering Research Laboratories (CERL). The CERL principal investigator was Dr. Donald M. Cropek. Walter J. Mikucki is Chief, CECER-UL-I; Dr. John T. Bandy is Laboratory Operations Chief, CECER-UL; and Gary W. Schanche is the responsible Technical Director, CECER-TD. The USACERL technical editor was William J. Wolfe, Technical Resources.

COL James A. Walter is Commander and Dr. Michael J. O'Connor is Director of CERL.

Contents

List of Tables and Figures

Tables

Figures

1 Introduction

Background

The armaments industry generates approximately 1600 tons per year of hazardous waste containing explosives and propellants, as a result of munitions production (Stratta 1993). By far, the most common disposal method for this hazardous waste is open burning/open detonation (OB/OD). This technique involves the destruction or burning of energetic materials (EM) and energetic waste (EW) in an open pit. Unfortunately, OB/OD has the potential to create environmental problems due to uncontrolled emission of by-products. Large scale experiments were conducted on OB/OD in an enclosed chamber known as a "bang box" (Johnson 1992). Extensive, real-time analytical measurements during these operations indicated a much smaller risk than expected. Nevertheless, the nonexhaustive nature of Johnson's experiments, together with the persistent negative perception of OB/OD, has fueled continued active research for alternative treatment methods. Currently, incineration is the most mature and well-characterized alternative disposal technology, and the method is already in use at several military installations. In the event that OB/OD is curtailed or even eliminated, studies examining incineration as a back-up treatment technology could have an immediate impact on mission readiness, especially if the focus of the work is on characterization and reduction of emissions.

Incineration, however, has its own poor reputation as a noxious pollution source. Despite trial burns that guarantee at least 99.99 percent destruction and removal efficiency of principal organic hazardous constituents (POHCs) (National Academy Press 1983), fear of both POHCs that pass through the system intact, and products of incomplete combustion (PIC), of which dioxin is the most notorious, limits public acceptance of incineration. The facts that incineration regulations specify and limit only POHCs, and that PIC can actually be more thermally stable than the parent compound (Graham, Hall, and Dellinger 1986), seem to justify concerns regarding incineration processes. It is imperative that the mechanisms for thermal decomposition/combustion during incineration be well studied under various operating conditions for all types of waste feeds. Incineration trial burns that would provide the required

data, however, are time consuming and expensive. Moreover, the release of contaminants to the environment during experiments where the outcome is unknown and the operating conditions are not optimized is unacceptable. A bench scale model of incineration, with tightly controlled analyses without inadvertent POHC or PIC release, is clearly a desirable solution. Unfortunately, other researchers have noted the difficulties (if not impossibilities) of completely characterizing the incineration process on the bench scale both qualitatively and quantitatively (Dellinger et al. 1986). These same researchers propose that the best possible results are limited to qualitative modeling.

Studies evaluating thermal degradation of municipal type waste in atmospheres of varying oxygen content have shown that PIC generated under very low or no oxygen content conditions best match the PIC generated during incineration of these same wastes (Tirey et al. 1991). It is postulated that POHCs are quickly and completely destroyed under conditions of excess oxygen, but that PIC are created in "pyrolytic pockets," that is, in areas of low or no oxygen content. Conclusions from this work support the use of laboratory scale pyrolysis to predict the PIC that may be emitted during incineration of municipal waste.

Pyrolysis / gas chromatography / mass spectrometry (PY/GC/MS) is a well known analytical technique typically used to study materials that are not amenable to direct injection into the GC/MS. Thermal decomposition of the recalcitrant material in the absence of oxygen (pyrolysis) can break the material down into gaseous fragments that immediately proceed into the GC/MS for separation and identification. Study of the fragment structures can provide intimate knowledge of the original material. PY/GC/MS has been used to examine such disparate samples as polymers, paints, oils, microorganisms, and soil (Wampler 1995). The same type of experimentation has been done on EM to benefit the military community.

Previous research has been driven by the belief that study of the thermal decomposition by-products and, hence, the decomposition mechanism, can contribute to an understanding of the relationship between molecular structure and explosive properties of EM. The ultimate goal of past work has been to use these results to devise and manufacture EM with greater stability and yet improved explosive characteristics. Studies of this kind include several combinations of a thermal decomposition method with an analytical technique for by-product identification. Of special interest are pyrolysis by a heated filament with mass spectral identification (Behrens 1990) and pyrolysis by a heated filament with infrared (IR) absorption (Oyumi and Brill 1986a). These two techniques have provided the greatest amount of information on EM

decomposition products. By-products from these two types of experiments provide the majority of entries on the literature reference lists given in later sections of this report. Other techniques are described in Ostmark, Bergman, and Ekvall (1992).

Instead of exploring mechanisms and ignition times, the definitive goal of this study was to assess the validity of using the pyrolysis chamber as a bench top model of a micro-incinerator, capable of operating under various conditions, but predominantly in the worst case scenario of an oxygen-deprived atmosphere. Laboratory PY/GC/MS on EM was done to uncover potential PIC from incineration of these same materials. To evaluate the success of PY/GC/MS to identify and predict PIC from EM incineration, it is essential to collect field samples during full-scale incineration of EM and compare this data to PY/GC/MS performed on the same EM. Clearly, pyrolytic PIC are not expected to exactly duplicate all incineration by-products, but positive matches between products from the two techniques would have several favorable consequences. Depending on how well the results match, use of PY/GC/MS as a model for an incinerator would be established. Success in this endeavor allows other tangents to follow. This method could determine how to optimize the incinerator, or conversely, determine the degree of pyrolysis occurring during the burn. Pyrolytic results could be used to determine worst-case by-products for new or untested waste feeds. This type of simple, fast, and inexpensive PY/GC/MS experiments can rapidly uncover proper incineration operating parameters, ascertain the required pollution control equipment, or even identify a marker PIC or POHC that could be used to assess system performance. Further experiments can also be performed to uncover special conditions or catalysts that could reduce or eliminate the formation of PIC.

Objective

The objective of this stage of work was to:

1. Perform pyrolysis on several types of energetic materials

2. Assess the scope of information that can be obtained by pyrolysis, gas chromatography, and mass spectrometry

3. Determine the effects of different pyrolysis parameters on the resultant set of by-products.

Future research will compare the by-product data generated here with data on PIC and POHCs collected from an energetic waste incinerator, to ascertain the usefulness of bench scale pyrolysis in modeling the incineration process. Planned research will investigate incineration by-products collected at Radford Army Ammunition Plant, Radford, VA.

Approach

1. A literature study was done and prior pyrolytic work was reviewed to compare and identify unknowns, and to pinpoint potential weaknesses in the experimental procedure.

2. Pyrolytic by-products were examined from a representative of three different types of explosives: nitramines (N-NO_2), nitroaromatics (C-NO_2), and nitrate esters (O-NO_2). The selected energetic materials (EM) were 1,3,5-trinitro-1,3,5-triazacyclohexane (RDX), 2,4,6-trinitrotoluene (TNT), and pentaerythritol tetranitrate (PETN), respectively. RDX was obtained from Redstone Arsenal, AL; TNT was obtained from Picatinny Arsenal, NJ; and PETN was obtained from Ensign-Bickford detonating E-cord (Chapter 3).

3. Several analytical laboratory configurations were set up at the Armament Research, Development, and Engineering Center (ARDEC), Picatinny Arsenal, NJ, and at the U.S. Army Construction Engineering Research Laboratories (USACERL) (Chapter 2).

4. Samples of RDX, TNT, and PETN were prepared (Chapter 2) and analyzed (Chapters 3, 4, and 5).

5. Results were analyzed and compared with work done in previous studies. Recommendations for further research were made (Chapter 6).

Scope

Results of this project apply to demilitarization activities of the U.S. Department of Defense, especially to hazardous waste incinerators operating on Industrial Operations Command installations. Further work may also examine the ability of PY/GC/MS to accurately represent conditions occurring during OB/OD operations.

Mode of Technology Transfer

It is anticipated that the information derived from this study will be incorporated into guidance for environmental representatives at military installations to help with decisions regarding demilitarization of energetic materials, pollution control, and environmental clean up.

2 Experimental Parameters

Energetic Materials

RDX was obtained from Redstone Arsenal, AL; TNT from Picatinny Arsenal, NJ; and PETN from Ensign-Bickford detonating E-cord. All of the energetic materials were military-grade condition and were used as received without further purification.

Equipment

A small pyrolysis chamber was installed on the injection port of a GC/MS. In this arrangement, the helium carrier gas flows through the chamber during pyrolysis and carries all gaseous by-products directly into the injection port of the GC. Several different instrument configurations were used in this study due to the division of labor between two laboratories and the availability of equipment. These configurations are described below and are listed in Table 1 for easy reference.

Configuration A (ARDEC Laboratory)

A CDS Pyroprobe 1000 was interfaced to the septum programmable injector (SPI) of a Varian Saturn 3 GC/MS. In Configuration A1, a PoraPLOT Q column from ChromPak, 25 m x 0.32 mm inside diameter (i.d.), was installed. This porous layer open, tubular (PLOT) column is made of a porous styrene-divinylbenzene homopolymer specializing in the separation of permanent light gases. This arrangement was available only for limited work.

Table 1. Experimental configurations for pyrolytic studies.

Configuration	Pyrolysis	GC	MS	Column
A1	CDS Pyroprobe 1000	Varian Saturn 3	Varian Saturn 3	PoraPLOT Q (25 m x 0.32 mm)
A2	CDS Pyroprobe 1000	Varian Saturn 3	Varian Saturn 3	PoraPLOT Q (25 m x 0.53 mm) + PoraPLOT Q (25 m x 0.32 mm)
B1	CDS Pyroprobe 121	HP GC 5890	HP MS 5970	HP 5 MS (25 m x 0.20 mm)
B2	CDS Pyroprobe 121	HP GC 5890	HP MS 5970	PoraPLOT Q (25 m x 0.32 mm)
B3	CDS Pyroprobe 121	HP GC 5890	HP MS 5970	PoraPLOT Q (50 m x 0.32 mm)

In Configuration A2, two PoraPLOT Q columns (25 m x 0.53 mm i.d. and 25 m x 0.32 mm i.d.) were connected using a capillary butt connector to obtain a better separation of CO and NO. This type of connector provided a better leak-free connection than the glass seal capillary column connectors. Initial pyrolysis studies showed that baseline separation of CO and NO was easily achieved at room temperature with the SPI pressure set to 7 psig.

GC Parameters. The injector and detector port temperatures were 250 and 280 °C, respectively. The GC oven program began at -20 °C for 5 minutes, then increased at 10 °C/min up to 220 °C, and was held for 33 minutes. The total acquisition time was 60 minutes. The SPI pressure was set to 7 psig, which was the optimum pressure at which to operate the SPI under cryogenic conditions. The ion trap settings were set to scan from 20 to 400 amu, with two mass scans per second. The automatic gain control (AGC) was on.

Pyroprobe Parameters. The CDS pyrolysis instrument is capable of controlling the pyrolysis temperature, the time interval, and the heating ramp. All of these parameters can be varied to determine the effects on the pyrolytic by-products. The chamber itself was maintained at 100 °C to ensure that the volatile gases would be swept into the GC and yet minimize sample degradation.

The CDS pyrolysis instrument also offered several probe options for pyrolyzing the sample. Pyrolysis may occur directly on a platinum ribbon or within a quartz tube or boat inserted into a platinum wire coil. With either the ribbon probe or the wire coil probe, the platinum element is resistively heated to a set temperature causing decomposition of the sample. Both pyrolysis techniques were evaluated, but use of the quartz tube wire coil probe was the usual method. When the quartz tube was used, quartz wool was added to hold the sample within the tube. Before introducing the sample, the platinum ribbon or quartz tube with wool was cleaned by heating to 1200 °C for 20 seconds, several times. After inserting a probe into the pyrolysis chamber, pyrolysis was not started for approximately 20 minutes to allow any entrant air to pass through the system.

Configuration B (USACERL Laboratory)

A Hewlett-Packard GC 5890 and MS 5970 electron impact (EI) mass spectrometer was interfaced with a CDS Pyroprobe 121. This instrumental setup was used with three different types of columns. In Configuration B1, the column was a HP-5MS column from Hewlett-Packard, 25 m x 0.2 mm i.d. x 0.33 mm film thickness. This column is a 5 percent phenyl, 95 percent methyl column designed for separation of heavier species. Configuration B2 changes the

column to a PoraPLOT Q column, 25 m x 0.32 mm i.d. As stated above, due to its unique adsorption characteristics, the PoraPLOT Q column can separate low molecular weight gases such as NO_x, CO_x, H_2O, etc. In Configuration B3, a longer PoraPLOT Q column, 50 m x 0.32 mm i.d., was used to achieve better separation of the light gaseous by-products.

GC Parameters. The injector and detector port temperatures were 250 and 280 °C, respectively. The GC injector was operated in the splitless mode. In Configuration B1, the GC oven temperature program was held initially at 50 °C for 5 minutes, then the oven temperature was ramped at 5 °C/minute up to 300 °C, and was held there for 15 minutes. The total acquisition period was 70 minutes. The mass analyzer was set to scan from 10 to 300 amu. In Configuration B2, the initial GC oven temperature was held at 40 °C for 1 minute, then the temperature increased to 120 °C at a rate of 50 °C/min. After 1.5 minutes at 120 °C, the temperature was increased to 200 °C at a rate of 20 °C/minute. After 4 minutes at 200 °C, the temperature was increased to 230 °C at 10 °C/minute and held for 14.9 minutes. The total run time was 30 minutes. Initially, the mass spectrometer acquired data from 10 to 120 amu. In later experiments, the upper mass limit was increased to 250 amu, but no additional peaks were detected. In Configuration B3, the GC temperature program was held at 40 °C for 3 minutes, then the temperature increased at 10 °C/minute up to 200 °C and held here for 52 minutes, for a total analysis time of 71 minutes.

Pyroprobe Parameters. These parameters were the same as those described above in Configuration A.

Sample Preparation

The EM was pyrolyzed either as a neat powder or dissolved in acetone. In either case, approximately 0.5 to 2 mg of EM was used in each experiment. When acetone was used as a solvent to introduce the EM onto a platinum ribbon or quartz tube containing quartz wool, the solvent was evaporated by heating the tube outside the pyrolysis chamber with a slow ramp from 60 to 110 °C.

3 1,3,5-Trinitro-1,3,5-triazacyclohexane (RDX)

Background

Nitramines have commanded a great deal of research attention. By far, the two most popular are 1,3,5-trinitro-1,3,5-triazacyclohexane (RDX) and 1,3,7-tetranitro-1,3,5,7-tetrazacyclooctane (HMX). This work uses RDX since it is one of the most important military high explosives, primarily because of its high stability and high explosive strength. RDX is also known as cyclotrimethylene-trinitramine, hexogen, or cyclonite. Figure 1 shows its structure.

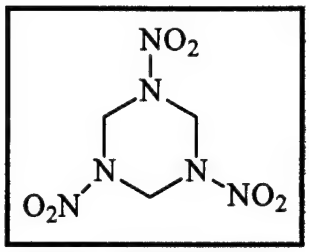

Figure 1. Structure of RDX.

RDX (MW = 222.6) has low solubility in water (0.006 grams of RDX / 100 grams of solvent at 25 °C), but good solubility in acetone (8.2 g / 100 g), dimethylformamide (37 g / 100 g) and dimethylsulfoxide (41 g / 100 g). Its melting point is 202 to 204 °C and its ignition temp is 229 °C (Yinon and Zitrin 1993). RDX is labeled as toxic to humans and has been used as a rodenticide, but its toxicity is limited due to poor solubility (Urbanski 1964a).

RDX exhibits lower stability and greater explosive power than TNT (Urbanski 1964a). Due to the high risk of accidental explosion, RDX is never handled in its pure form, but either desensitized with additives or mixed with water or solvents. RDX is used for booster charges and in mixtures with other explosives. It is probably best known as a component of Semtex, a plastic explosive, together with PETN (Yinon and Zitrin 1993).

Several reports agree on the particular permanent light gases and smaller organic by-products that are pyrolytically produced from RDX. Analytical techniques for the identification of these by-products include fast Fourier transform infrared absorption (FTIR) (Oyumi and Brill 1985; Botcher and Wight 1993), mass spectrometry (Snyder et al. 1990; Behrens and Bulusu 1992; Ostmark, Bergman and Ekvall 1992), GC/MS (Hoffsommer and Glover 1985),

coherent anti-Stokes Raman scattering (CARS) (Aron and Harris 1984), and GC (Huwei and Ruonong 1989). Pyrolytic methods include laser-induced decomposition (Botcher and Wight 1993; Ostmark, Bergman and Ekvall 1992), heated filament (Oyumi and Brill 1985; Snyder et al. 1990; Huwei and Ruonong 1989), heated block (Behrens and Bulusu 1992; Hoffsommer and Glover 1985; Behrens 1990), and flame combustion (Aron and Harris 1984). The dominant by-products and their production pathways are comprehensively described by Schroeder (1981). Table 2 lists previously observed by-products from the pyrolysis of RDX in order of increasing molecular weight. Note that none of the references observed all of the by-products. Except for HCN and NO_2, the by-products observed most often were also observed by Rideal and Robertson (1948) during the analysis of by-products from the thermal decomposition of RDX. Their analytical results for the thermal decomposition of RDX are described by the following equation:

$$C_3H_6N_6O_6 = 0.75NO + 0.76N_2O + 1.03N_2 + 0.44CO_2 + 0.29CO + 0.06H_2 + H_2O + CH_3O + residue$$

Other by-products are frequently identified by only a single reference depending on pyrolysis method and the sophistication of the analytical technique. The species listed in this table will help identify the by-products observed in this work.

Table 2. Reference list of previously observed by-products from the pyrolysis of RDX.

Common Name	Molecular Formula	Molecular Weight	Reference
Hydrogen	H_2	2	1, 2
Methane	CH_4	16	1
Ammonia	NH_3	17	2
Water	H_2O	18	2, 3, 4, 5
Hydrogen cyanide	HCN	27	1, 2, 3, 4, 6, 7, 8
Nitrogen	N_2	28	1, 2, 4
Carbon monoxide	CO	28	1, 2, 3, 4, 6, 8
Formaldehyde	H_2CO	30	1, 2, 3, 4, 5, 6
Nitric oxide	NO	30	1, 2, 3, 4, 5, 6, 7, 8
Oxygen	O_2	32	1
Ring fragments	$N(CH_2)N$, $(CH_2)_2N$	42	4
Imine compound	CH_2NCH_2	43	9
	HOCN	43	4
Hydrogen isocyanate	HNCO	43	6
Carbon dioxide	CO_2	44	1, 2, 4, 6, 7, 8
Nitrous oxide	N_2O	44	2, 3, 4, 5, 6, 8
Formamide	$CHONH_2$	45	3, 9
Formic acid	HCOOH	46	2
Nitrogen oxide	NO_2	46	2, 3, 4, 5, 6
	HONO	47	3, 6, 8

Common Name	Molecular Formula	Molecular Weight	Reference
Nitrogen oxide	NO_2	46	2, 3, 4, 5, 6
	HONO	47	3, 6, 8
Ethanedinitrile	$(CN)_2$	52	4
N-nitrosoformimine	CH_2NNO	58	2, 3
N-methylformamide	$CHONH(CH_3)$	59	3, 5, 9
Acetaldoxime	CH_3CHNOH	59	9
Nitromethane	CH_3NO_2	61	4
Oxadiazole	$C_2H_2N_2O$	70	4
	$CH_2NCH_2NCH_2$	70	8
N,N-dimethylformamide	$CHON(CH_3)_2$	73	3
N-nitroformimine	CH_2NNO_2	74	2
Dimethylnitrosoamine	$(CH_3)_2NNO$	74	5
N-hydroxy-N-methylformamide	$CHONH(CH_2OH)$	75	2
1,3,5-Triazine	$C_3H_3N_3$	81	4
N,N-dimethylaminoacetonitrile	$(CH_3)_2NCH_2CN$	84	9
Ring fragments	$(CH_2)_2NNO_2$	88	4
Nitrogen dioxide	N_2O_4	92	7
Oxy-s-triazine	$C_3H_3N_3O$	97	3, 5
	$(CH_3NHCHO)_2$	118	3
	$C_2H_4N_2(NO)NO_2$	132	3
Trinitroso RDX	$C_3H_6N_6O_3$	174	10
Dinitroso RDX	$C_3H_6N_6O_4$	190	10
Mononitroso RDX	$C_3H_6N_6O_5$	206	3, 5, 10

[1]Aron and Harris 1984
[2]Schroeder 1981
[3]Behrens and Bulusu 1992
[4]Ostmark, Bergman, and Ekvall 1992
[5]Behrens 1990
[6]Oyumi and Brill 1985
[7]Botcher and Wight 1993
[8]Huwei and Ruonong 1989
[9]Snyder et al. 1990
[10]Hoffsommer and Glover 1985

Results

Table 3 lists the light molecular weight by-products obtained from pyrolyzing neat RDX on a platinum ribbon using Configuration A2. The results from five different pyrolysis temperatures, from 300 to 900 °C, are shown. The holding time at these pyrolysis temperatures was 10 seconds. The compounds can be broken down into two fractions. Fraction I consists of all compounds that elute before water on the PoraPLOT column, inclusive of water. This fraction contains the light permanent gases such as NO, CO, CO_2, and N_2O. Fraction II contains all other by-products that elute after water and tend to be the higher molecular weight species, C_2 and above. This table can help determine the

Table 3. By-products from the pyrolysis of RDX on a platinum ribbon using Configuration A2.

Molecular Formula / Common Name	300 °C	400 °C	500 °C	700 °C	900 °C
Fraction I					
NO,CO	9.5*	12.6	28.0	37.4	30.7
CO_2	3.8	8.5	15.7	15.6	56.2
N_2O	23.0	24.7	24.2	26.8	4.9
H_2O	0	2.1	1.0	4.6	3.8
Fraction II					
HCN	0	0	0	1.7	0
H_2CO	0	0.4	0	1.2	3.7
H_2CN_2H	0	4.8	8.7	0.5	0
NH_2COH	63.7	37.0	10.1	5.7	0
Triazine	0	4.8	5.3	2.6	0
HCOOH	0	4.7	7	3.9	0

* All values expressed as a percent of the total peak area of the pyrogram.

pyrolytic by-products that are more stable. Higher pyrolytic temperatures are expected to induce a more complete breakdown of EM into its final end-products. The table shows that, as the pyrolysis temperature increases, the relative amount of Fraction I species increases at the expense of the relative amount of Fraction II species. But up to 700 °C, the total number of Fraction II species observed actually increases.

Carbon dioxide (CO_2) illustrates the behavior of a final end-product. As the pyrolytic temperature increases, the relative fraction of CO_2 increases, indicating that CO_2 is a stable end product for carbon and possibly even oxygen. On the other hand, although N_2O increases in abundance up to 700 °C, its abundance rapidly decreases at 900 °C. Therefore, N_2O is not the most stable end product for nitrogen. The only other possible nitrogen end products are HCN, NO and N_2. The concentration of HCN produced is too low to account for all the nitrogen from RDX and its abundance drops to zero at higher temperatures. It is difficult to determine the exact behavior of NO and N_2 since they co-elute with CO. Since the abundance of CO_2 increases so dramatically as the pyrolysis temperature increases, it is postulated that the contribution of CO to the NO/CO/N_2 peak will diminish until this peak is due solely to nitrogen-containing gases. In addition, as the abundance of N_2O decreases, the NO/N_2 peak will increase to account for this nitrogen as well. Diatomic hydrogen, H_2, was not observed due to its low mass, but this gas, together with H_2O, are major end products for hydrogen.

At a pyrolysis temperature of 300 °C, formamide (NH_2COH) is the only Fraction II species present. It is also the largest Fraction II component at all other pyrolysis temperatures except 900 °C. Curiously, Schroeder does not list formamide as a pyrolytic end product by any mechanism (Schroeder 1981). Behrens and Bulusu identify formamide as a liquid phase decomposition product of RDX during breakdown of the polyamide residue, but only in the presence of a catalyst with the co-production of formaldehyde (Behrens and Bulusu 1992). The production of formaldehyde clearly does not track the production of formamide. At 900 °C, only formaldehyde remains, indicating that it may also be a stable carbon end product. Hydrogen cyanide is present only at 700 °C; its contribution is surprisingly small based on previous work. Triazine and formic acid were also detected although they have been only rarely seen in the literature.

Most curious is the peak tentatively identified as H_2CN_2H, with a molecular weight of 43. This species has not been previously observed, but it is probably a ring fragment similar to those listed in Table 2 with molecular weights of 42 and 43.

Using Configuration A2 with neat RDX in a quartz tube, the relative abundances of by-products from pyrolysis were measured and listed in Table 4. The samples were pyrolyzed for 10 seconds. The same general behavior is noted as in Table 3; that is, the relative abundance of Fraction I species dominates at all pyrolysis temperatures and the total amount of Fraction II species decreases as the pyrolysis temperature increases. In Fraction I, the abundance of CO_2 steadily increases at all temperatures as expected for this primary carbon end-product, while the abundances of N_2O and NO/CO again have the same increase at intermediate pyrolysis temperatures followed by a decrease at the highest

Table 4. By-products from the pyrolysis of RDX in quartz tube using Configuration A2.

Molecular Formula / Common Name	300 °C	400 °C	700 °C	900 °C
Fraction I				
NO, CO	20.0[a]	34.1	39.1	37.4
CO_2	8.1	8.0	12.2	30
N_2O	46.7	47.1	41.8	24.6
H_2O	0.3	0.3	0.1	5.6
Fraction II				
HCN, CH_2O	10.0	2.1	2.0	1.9
CH_3COH	1.2	3.1	0.9	0.4
NH_2COH	2.8	1.4	1.9	0
Triazine	5.8	1.4	1.9	0
CH_3NHCOH	5.0	2.5	0.1	0

[a] All values expressed as a percent of the total peak area of the pyrogram.

temperature. Again, the NO/CO peak most likely has a significant contribution from N_2. In Fraction II, the hydrogen cyanide, formaldehyde, formamide, and triazine are again present, most notably at 300 °C. N-methylformamide (CH_3NHCOH) is new to these experiments, but has been observed by others. The presence of acetaldehyde (CH_3COH) is unexpected and unprecedented.

A comparison of Tables 3 and 4 illustrates three general differences between pyrolysis directly on a platinum ribbon and pyrolysis in a quartz tube. First, the total amount of Fraction I produced at any given pyrolysis temperature is greater using a quartz tube. Second, the variety of Fraction II by-products is quite different. The platinum ribbon method produced ring fragments and formic acid while the quartz tube method instead produces acetaldehyde and N-methylformamide. Third, the platinum ribbon produces only one Fraction II product, formamide, at 300 °C, but produces an increased number of Fraction II by-products as the pyrolysis temperature increases to 700 °C while the quartz tube method produces the same species throughout the temperature series.

Several factors may help to explain these differences. The first factor is the difference in the thermal behavior of the platinum ribbon versus the quartz tube. The quartz tube is placed within the coil of a platinum wire. When the wire is resistively heated, the sample within the quartz tube begins to experience a temperature change. But since the quartz has a nonzero thermal resistivity, the sample temperature will lag behind the wire temperature and ultimately may not even reach the desired pyrolysis temperature. This has been noted in experiments where the pyrolysis hold time was brief and little, if any, pyrolysis occurred. If the hold time is too short this temperature lag phenomenon can have the net effect of lowering the actual pyrolysis temperature experienced by samples within the quartz tube and sets an upper limit to the pyrolysis ramp rate. If the sample is pyrolyzed at this lower actual temperature, the relative amount of Fraction I products should be smaller in favor of a greater total amount of Fraction II products. Since the opposite behavior is observed, this effect is not crucial because the holding time was long enough to ensure reasonable equilibration between the coil temperature and the sample.

A sample placed directly on the platinum ribbon can have the opposite problem. Since the platinum metal responds quickly when current is applied, EM on the ribbon may experience a shock due to the rapid temperature change. In addition, it is possible that the ribbon temperature will overshoot the desired pyrolysis temperature due to the noninstantaneous response of the metal when reaching the desired pyrolysis temperature. Both effects serve to impart more

energy to the sample and to cause a more complete pyrolytic breakdown. This higher effective temperature should increase both the relative amount of Fraction I components and the variety of Fraction II products. Again, the results do not follow this pattern. Thus, this factor also seems to be relatively unimportant.

A more important difference between the tube and the ribbon is the residence time of the sample and its by-products within the pyrolytic hot zone. The quartz tube and the wool provide a more enclosed region for the sample. By-products can be trapped and pyrolyzed for a longer time before being swept out of the tube. This additional time causes further breakdown of by-products. The net result is a greater amount of Fraction I light gases and a lower total amount of Fraction II by-products as compared to platinum ribbon results. A gaseous by-product produced on the platinum ribbon can immediately leave the hot metal surface and will not undergo further pyrolytic breakdown. This is indeed the pattern observed at all temperatures in Tables 3 and 4, but is especially pronounced at the lower temperatures. Data in Table 3 suggest that formamide is an example of a species that evolves immediately from the platinum ribbon, but is easily broken down into other species when trapped in the quartz tube. This behavior could be exploited to distinguish between initial pyrolytic reactions and secondary reactions that cause further by-product degradation.

Another experimental factor to be considered is the catalytic nature of platinum metal. When the sample is placed directly on the platinum metal, it is possible that alternate degradation pathways are enhanced. This can lead not only to changes in the relative abundances of by-products, but can also create completely different chemical species. Clearly, the platinum ribbon may have a major influence on the pyrolytic mechanism. This could explain the appearance of ring fragments in Table 3. Also, as noted above, formamide was observed only in the presence of a catalyst (Behrens and Bulusu 1992). The results obtained here do not strictly support this observation since, although formamide is the dominant Fraction II by-product using the platinum ribbon, it was also observed to a lesser extent with the quartz tube. Quartz tubes are thus preferred to minimize effects that are not strictly pyrolytic in nature. The influence of the platinum ribbon could be exploited, however, when pyrolysis is used for characterization of difficult unknown samples. By providing complementary information to quartz tube fragmentation, elucidation of chemical structures would be enhanced.

Figure 2 shows a pyrogram of RDX collected using Configuration B2 with a pyrolysis set point of 500 °C. Note the greater number of by-products in this

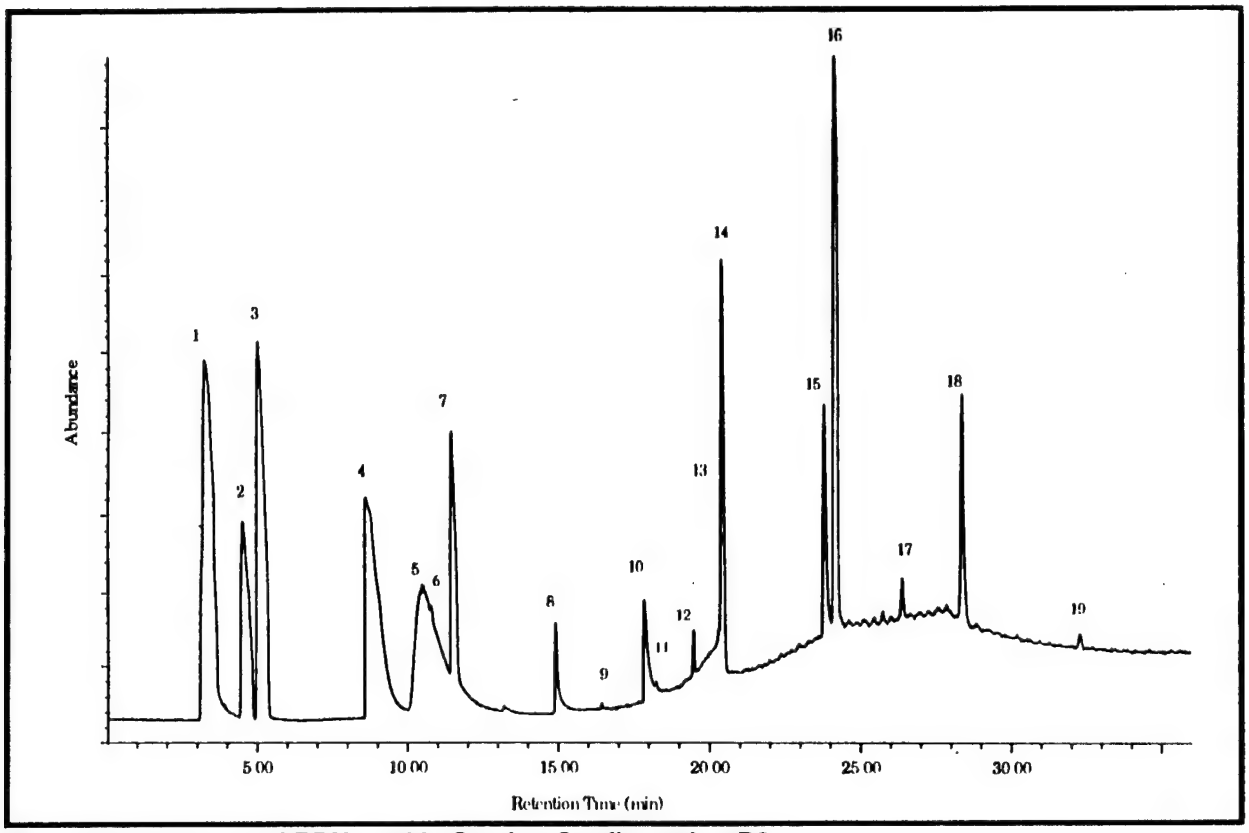

Figure 2. Pyrogram of RDX at 500 °C using Configuration B2.

pyrogram than seen using Configuration A. This increased wealth of data proved to be a typical pattern distinguishing the two configurations. Further, more by-products are observed in this data than are observed in any other single reference in Table 2. The numbered peaks correspond to the peak identifications listed in Table 5. Peak 1 comprises the coeluting light gases, N_2, NO, and CO. Peaks 2, 3, and 4 represent the remaining Fraction I components, CO_2, N_2O, and H_2O, respectively.

Several different Fraction II by-products build off the structure of formaldehyde. Formaldehyde (peak 5) is a very broad peak eluting just after water. Peaks 9 and 10 are methyl formate and formic acid, respectively. Methyl formate, although quite small, is noteworthy specifically because it is not listed as a known RDX by-product in Table 2.

Formamide (15), N-methylformamide (17) and N,N-dimethylformamide (18) have all been noted before; however, it is interesting that formamide and N,N-dimethylformamide are more abundant than N-methylformamide. The progression from N,N-dimethylformamide to N-methylformamide to formamide occurs by a successive loss of a methyl group. The peak ratios of these three

Table 5. Pyrolytic by-products from RDX using Configuration B2 at 500 °C. The peak numbers correspond to the peaks labeled in Figure 2.

Peak	Molecular Formula / Common Name	Mass Spectra Peaks
Fraction I		
1	NO, CO, N_2	28,14,12
2	CO_2	44
3	N_2O	46
4	H_2O	18
Fraction II		
5	HCHO	30,29,28,14,13,12
6	$(CN)_2$	52,38,26,24,15,12
7	HCN	27
8	CH_2=NCH_3?	43,42,29,28,15
9	Methyl formate	60,32,31,29,28,27,15
10	Formic Acid	46,45,44,29,28,18,17
11	Acetonitrile	41,40,39,38,14,12
12	Acetone	58,43,42,29,27,15,14
13	Nitromethane	61,46,30,27,15
14	Unknown	70,43,42,41,40,29,28,27
15	Formamide	45,44,43,29,27,17,16
16	Triazine	82,81,54,53,40,39,38,28,27,26,12
17	N-methylformamide	59,58,30,29,28,27,15
18	N,N-dimethylformamide	73,45,44,43,42,29,28,27,17,16
19	Unknown	106,80,54,53,52,38,28,27

compounds are expected to either increase or decrease in this same progression. Since the abundance of N-methylformamide is the smallest of the three, this species is the most thermally labile, quickly breaking down to formamide or smaller products.

Acetonitrile (11) is small and is not listed as a by-product on Table 2, but its presence is not unreasonable since several aminoacetonitriles are listed. Acetone (12) is an appreciably sized peak, also previously unobserved; however, it is possible that this is the remains of an RDX production solvent especially since concerted efforts were not taken to thoroughly dry the RDX prior to pyrolysis. Peak 13 is merely a shoulder on a major peak, but with background subtraction, a good library match is obtained with the seldom noted compound nitromethane. HCN (7) and triazine (16) are the last two positively identified species. Both have been previously documented as major by-products.

Peaks 6, 8, 14, and 19 produced only ambiguous library matches. Table 5 lists the mass peaks for these unknown species. Although peak 6 registers as only a very small peak co-eluting with formaldehyde, its mass spectra is easily

extracted by background subtraction. With the assumption that m/z = 52 is the molecular ion peak, a match with ethanedinitrile, $(CN)_2$, is probable. This species is observed from pyrolysis of all three EM studied here. Peak 8 is large with its heaviest mass fragment at 43 amu. Assuming that 43 amu is the molecular ion peak, hydrogen isocyanate, HN=C=O, is an unlikely match due to its inability to account for the major daughter peak at 29 amu, while HOCN cannot account for the peak at 15 amu. Pyrolysis of other EM has produced a peak in the same region as peak 8, which might provide a clue to its identification. Figures 3a and 3b show this region of the pyrogram for both RDX and PETN, respectively. The retention times are slightly different, 14.9 minutes for peak 8 versus 15.5 minutes for the PETN by-product. Note the skewed appearance of peak 8 versus the symmetrical shape of the peak produced from PETN. This may indicate a different structure for the two species. The mass spectra for peak 8 and the PETN by-product are shown in Figures 3c and 3d, respectively. The PETN by-product has a large molecular ion peak at 44 amu and its mass spectrum is virtually indistinguishable from the mass spectra of both ethylene oxide and acetaldehyde. The mass spectrum of peak 8 has similar mass fragments at 15, 29, 42, 43 amu, but the ratios are completely different and the m/z = 44 is completely missing. Based on these discrepancies, peak 8 is neither ethylene oxide nor acetaldehyde, which agrees with their absence from Table 2. The only possibility remaining from Table 2 is the imine compound, CH_2NCH_3, a ring fragment. Based on earlier discussions regarding the platinum ribbon versus the quartz tube, it would be instructive to use the platinum ribbon to pyrolyze RDX via Configuration B2 to determine if this ring fragment peak increases.

Peak 14 is the unknown of greatest concern due to its large abundance. Several researchers have noted a peak with a parent ion of 70 amu and the several possibilities proffered are shown in Table 2. The compound $CH_2NCH_2NCH_2$ is attractive since it is easily derived as a ring fragment from RDX and is a systematic extension of the possible structure given for peak 8 above. The only hit from the MS library is methylaminoacetonitrile, which is not completely unreasonable given that these types of compounds have been previously observed and acetonitrile is seen here. Peak 19 is small and has a parent ion peak of 106 amu. The best library match is ethenyl pyrazine. This is interesting since, aside from triazine, it is the only other species produced that retains a ring structure. The reasoning that argues against this identification is the major rearrangement required to obtain this structure from the cyclohexamine structure. In addition, this species has not been previously observed.

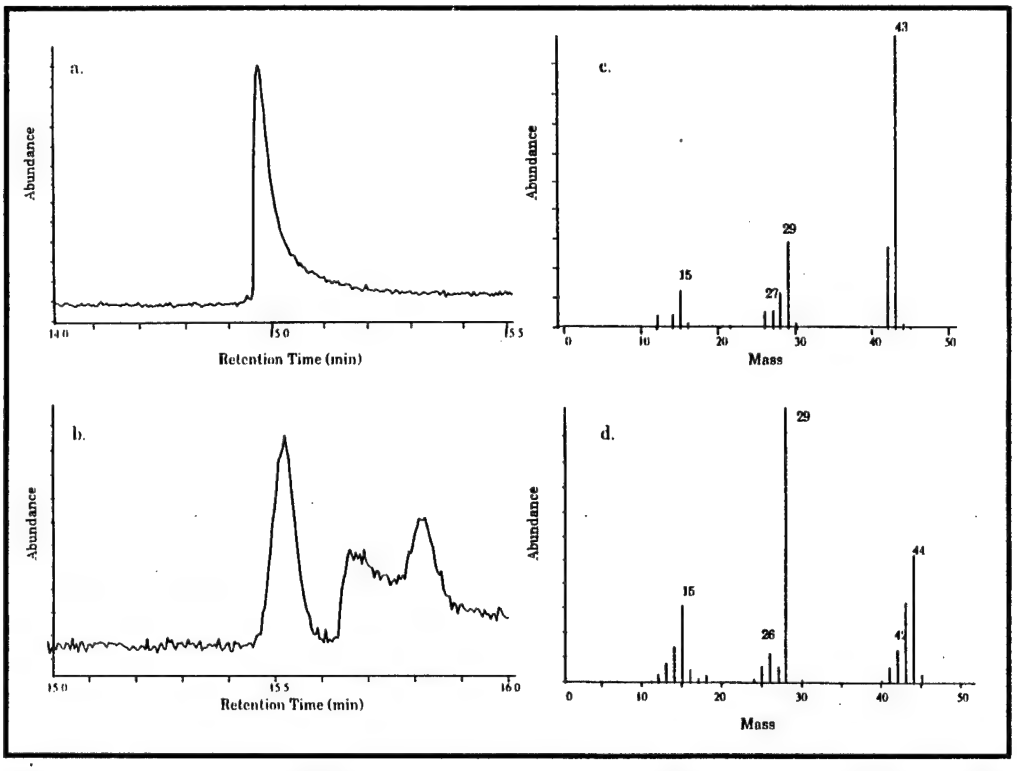

Figure 3. Comparison of pyrolytic by-products from RDX and PETN. A slice of the pyrogram is shown for (a) RDX by-product, peak 8 from Figure 2 and (b) PETN by-product with a similar retention time, and the mass spectra for (c) the RDX by-product and (d) the PETN by-product.

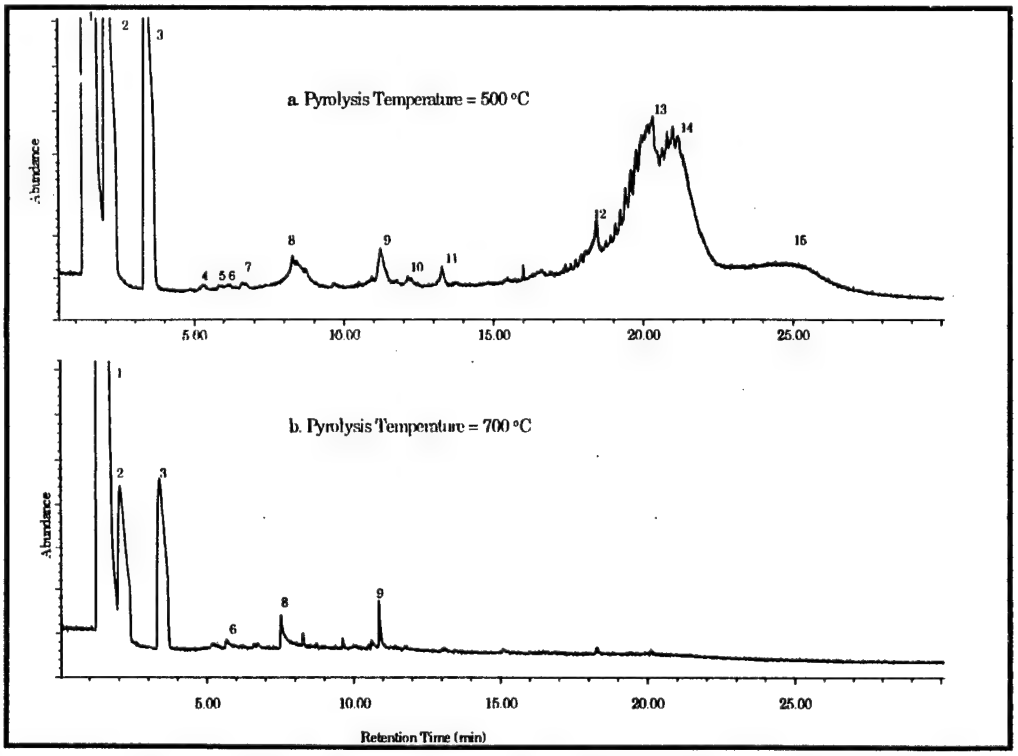

Figure 4. Pyrogram of RDX using Configuration B1 at (a) 500 °C and (b) 700°C.

Figures 4a and 4b show the pyrograms of RDX using Configuration B1 with pyrolysis set temperatures of 500 and 700 °C, respectively. These two pyrograms are on the same abundance scale for direct comparison. This type of experiment is designed to study the higher molecular weight by-products from pyrolysis. In these figures, peaks labeled with the same number have the same mass spectra and retention times and are thus equated as identical by-products. The light molecular weight gases elute quickly as an unresolved peak (peak 1) between 1 and 2 minutes. Peak 2 is the unknown with a molecular weight of 70 amu; peak 3 is 1,3,5-triazine. Both were previously observed in Table 5 as peaks 14 and 16, respectively. As expected, the absolute amounts of these two species, as well as all other by-products, decrease as the pyrolytic temperature increases from 500 to 700 °C. The total number of peaks also decreases as the pyrolysis temperature is increased. The higher temperature induces a more complete destruction of Fraction II by-products, converting these into Fraction I species.

The peaks 4 through 15 observed in Figure 4 are quite small and identification expectations are low. Suitable library matches were obtained for peaks 4 (dimethylnitrosoamine), 5 (aminopyrazine), 6 (N-methylformamide), and 7 (N-formyl-N-methylformamide), but these peaks are so small that attempts to unequivocally label these as by-products is premature at best.

Peak 8 is N,N-dimethylformamide, which was also observed in Figure 2, and peak 9 is identified as oxy-s-triazine (major mass peaks at m/z = 97, 81, 70, 54, 43, 40, 28, and 27). Peak 10 (major mass peaks at m/z = 113, 85, 55, 43, 29, and 28), peak 11 (major mass peaks at m/z = 96, 73, 45, 30, 29, and 28), and peak 12 (major mass peaks at m/z = 100, 42, and 30) remain unidentified.

The broad peaks 13, 14, and 15, illustrate a different problem. The mass spectra for these peaks consist primarily of small, light fragments. The mass spectra for peaks 13 and 14 are shown in Figures 5a and 5b and the broad shoulder labeled as peak 15 is shown in Figure 5c. Based on the similarity of the mass spectra, the compounds giving rise to peaks 13 and 14 have a similar structure, but the lack of a molecular ion peak is troubling. These pyrolytic by-products are degrading either on-column or, more likely, during electron ionization, preventing characterization. Considering that RDX has the same degradation problem, peaks 13 and 14 may be compounds that are very similar in structure to RDX, such as the nitroso-RDX species listed in Table 2, or even undegraded RDX itself. All three of these by-products are completely destroyed when subjected to the higher pyrolytic temperature.

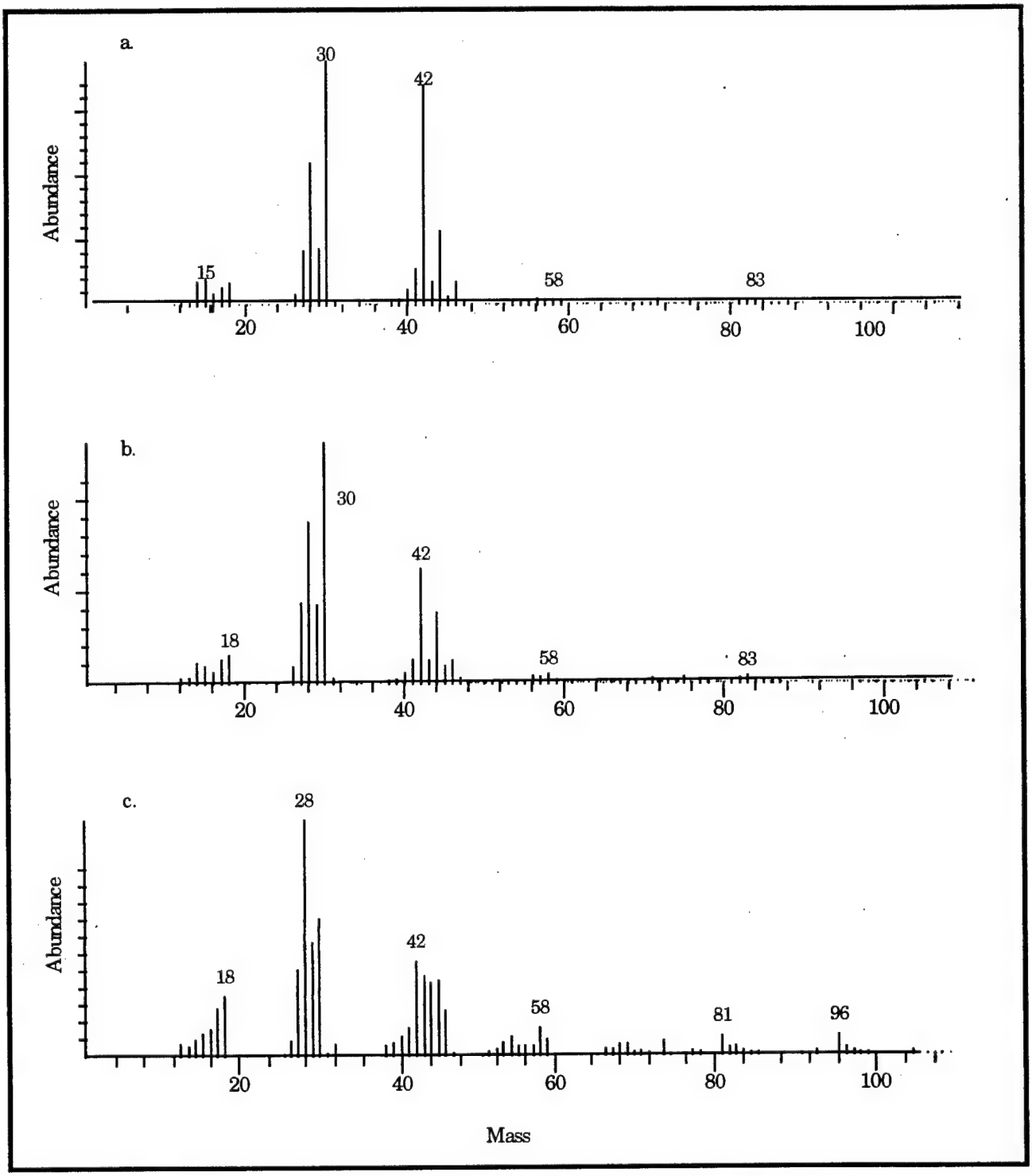

Figure 5. Mass spectrum of (a) peak 13, (b) peak 14, and (c) peak 15 from Figure 4a.

4 2,4,6-Trinitrotoluene (TNT)

Background

2,4,6-Trinitrotoluene (TNT) is the most widely used energetic compound. This representative from the nitroaromatic class of EM is popularized by several desirable characteristics. TNT has high stability and low sensitivity to impact, friction, and high temperature. It is used for both commercial and military applications and is a good sensitizer. Figure 6 shows its structure.

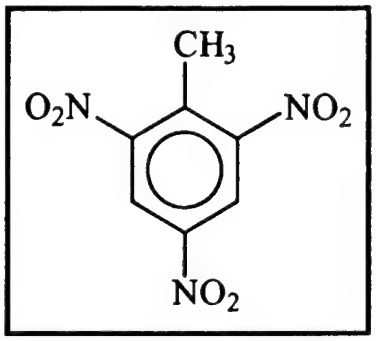

Figure 6. Structure of TNT.

TNT (MW = 227.1) has low solubility in water (0.02 grams of TNT / 100 grams of water at 25 °C), a trait exploited during production to separate it from unwanted isomers. Other solvents that are better for TNT include benzene (88 g / 100 g), dimethyl sulfoxide (128 g / 100 g), acetone (132 g / 100 g), and dimethylformamide (142 g / 100 g). Its melting point is 80.65 °C and its ignition temperature is 300 °C (Yinon and Zitrin 1993). TNT is toxic. Its most marked symptom is a decrease in red blood cells and hemoglobin (Urbanski 1964b).

Table 6 lists the by-products that have been observed on thermal degradation of TNT. In contrast with Table 2 of RDX by-products, the lack of permanent gases and lighter weight by-products is immediately evident. Most likely, the literature search may have missed relevant articles that focus on the pyrolysis of TNT. The references listed here study thermal decomposition at lower temperatures (300 °C) than typically used in pyrolysis. Higher temperature studies use either mixtures of TNT with other EM or TNT contaminated waste, making it difficult to isolate by-products solely due to TNT. For example, Volk (1990) and Knight (Knight and Elston 1978) both observed H_2, CH_4, CO, CO_2, N_2, NO, HCN, C_2H_2, NH_3, H_2O, and solid carbon residues from thermal decomposition of materials that contain TNT. Knight and Elston also observed ethane, propane, propylene, butane, and butenes. Many of these species no doubt originated from the TNT. From Table 6, the majority of the by-products are in the solid phase during decomposition and arise from progressive steps in the oxidation of the methyl group. Unlike RDX, thermal degradation of TNT

has the ability to create larger species than TNT itself. The dimer products that have been observed result from the creation of radicals at either the methyl group or the para nitro group.

Table 6. Reference list of previously observed by-products from the pyrolysis of TNT.

Common Name	Molecular Weight	Structure	Reference
Hydrogen cyanide	27	HCN	1
Nitrogen	28	N_2	1
Carbon monoxide	28	CO	1
4,6-Dinitroanthranil	209.1	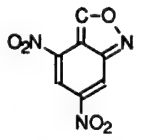	2,3,4
1,3,5-Trinitrobenzene	213.1	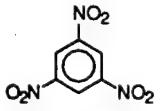	3,4
2,4,6-Trinitrobenzaldehyde	241.1	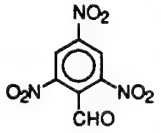	2,3
2,4,6-Trinitrobenzyl alcohol	243.1	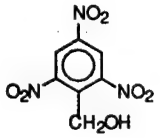	2,3,4
2,4,6-Trinitrobenzoic acid	257.1	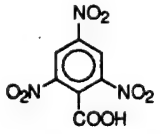	3,4
Azoxy compound	406.1	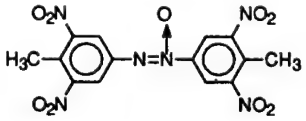	2,3
Dimer compound	423.7	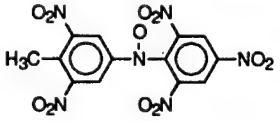	5

[1] Blais, Greiner, and Fernandez 1990
[2] Dacons, Adolph, and Kamlet 1970
[3] Shackleford 1990
[4] Rogers 1967
[5] Menapace and Marlin 1990

Results

Using Configuration A1, Table 7 lists the by-products obtained from the pyrolysis of TNT at 400 and 700 °C. At 400 °C, CO_2 and H_2O are the only Fraction I by-products present. It is curious that there are no nitrogen-containing Fraction I by-products. This may indicate that the fracture of the C-N bond is not the initial primary step in the degradation mechanism, but instead, internal rearrangement and ring fragmentation occurs producing Fraction II species which incorporate the nitrogen. In fact, pyrolysis of TNT seems to favor formation of the C≡N bond, which is present in many Fraction II by-products. Note that identification of two ring fragments, $H_2C_2N_2$ and C_5H_4N, is tentative while two major by-products remain unidentified. The lack of raw data has hindered further analysis of these peaks. Ethanedinitrile, $(CN)_2$, is again produced, but is more prominent from TNT than from RDX decomposition.

At 700 °C, the temperature is high enough to break down Fraction II by-products to nitrogen-containing Fraction I by-products. Unlike RDX, N_2O is never an appreciable product. All nitrogen appears in Fraction I as NO (or N_2).

Pyrolysis at 300 °C was attempted, but no decomposition products were observed. This is expected since the ignition temperature of TNT is 300 °C and the TNT within the quartz tube most likely experienced a slightly lower pyrolytic temperature than this setpoint. It has been shown that early decomposition reactions result in the evolution of little gas (Rogers 1967). Therefore, at 300 °C, the majority of by-products will be localized in the nonvolatile TNT solid phase.

Table 7. By-products from pyrolysis of TNT using quartz tube and wool at 400 °C and 700 °C using Configuration A1.

Molecular Formula / Common Name	400 °C	700 °C
Fraction I		
NO, CO	0*	49.6
CO_2	57.3	40.7
N_2O	0	0.4
H_2O	9.8	1.8
Fraction II		
$(CN)_2$	10.9	1.4
HCN	3.4	3.8
Unknown	5.2	1.1
CH_3CN	0	0.4
$H_2C_2N_2$	0	0.4
Unknown	11.9	0
C_5H_4N	1.5	0.4

* All values expressed as a percent of the total peak area of the pyrogram.

This laboratory repeated several experiments on TNT using Configuration B2. Figures 7, 8, 9, and 10 show pyrograms of TNT resulting from pyrolysis set temperatures of 400, 500, 600, and 900 °C, respectively. The 500 °C pyrolytic results of Figure 8 consist of pyrograms using four different masses of TNT. Unlike RDX, pyrolysis of TNT below 600 °C was relatively uneventful. At the lowest pyrolysis temperature, 400 °C, little pyrolytic behavior was noted even though the pyrolysis temperature was well above the ignition temperature of TNT. Analysis of the residue from this experiment would be quite instructive and likely contains many of the decomposition products from Table 6. Peak 1 in Figure 7 has no mass peak at either 12 or 30, but instead consists of peaks at 14, 16, 28, and 32 amu. This indicates the lack of CO and NO and the presence of N_2 and O_2. Peaks 2 and 3 are CO_2 and H_2O, respectively. Methanol (peak 4) and methyl formate (peak 5) are unusual. These two species are observed at 400 and 900 °C and only at the lowest TNT mass pyrolyzed at 500 °C, but not at 600 °C. If these species are easily formed pyrolysis products, the concentration trend should either progressively increase or decrease in response to the pyrolysis temperature. In addition, production of these two compounds should increase with an increasing mass of TNT pyrolyzed at any particular temperature. Since neither of these behaviors is observed, methanol and methyl formate are not pyrolysis products, but are instead solvent remains from processing and handling of TNT. Sample inhomogeneities can account for discrepancies between pyrograms. This also lends credence to the hypothesis of a contaminant presence rather than a pyrolysis product.

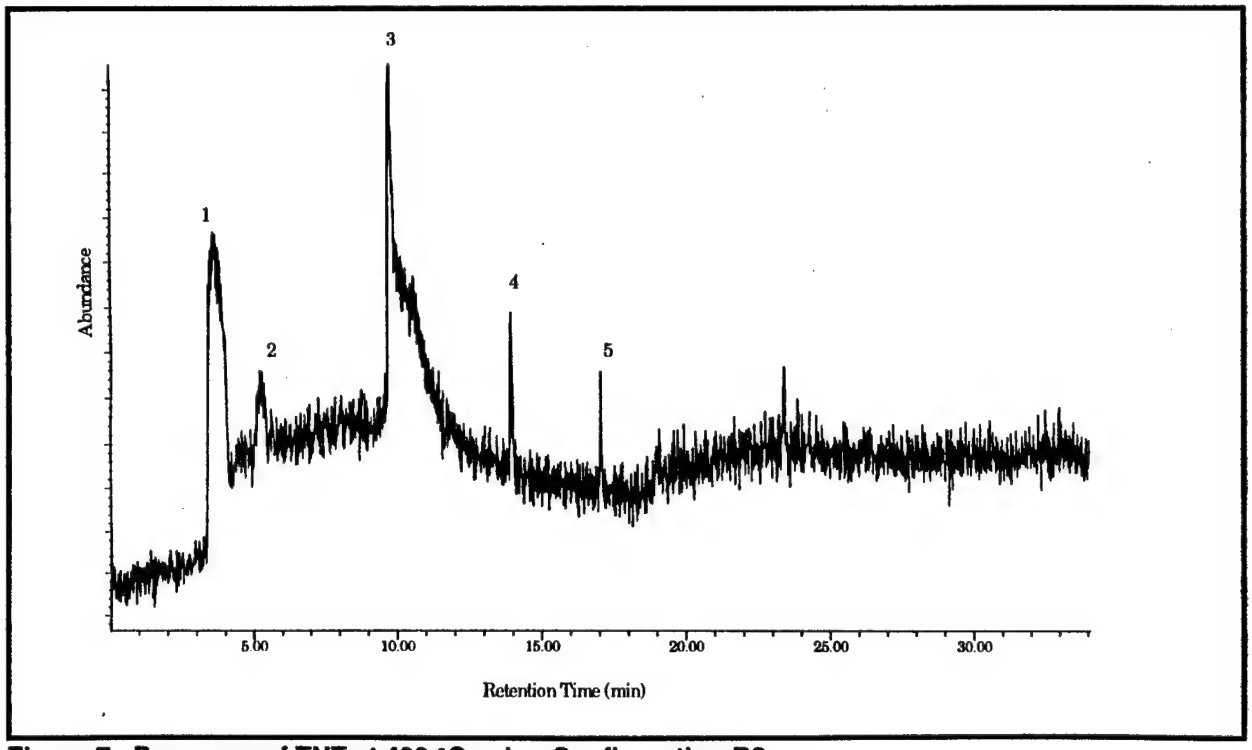

Figure 7. Pyrogram of TNT at 400 °C using Configuration B2.

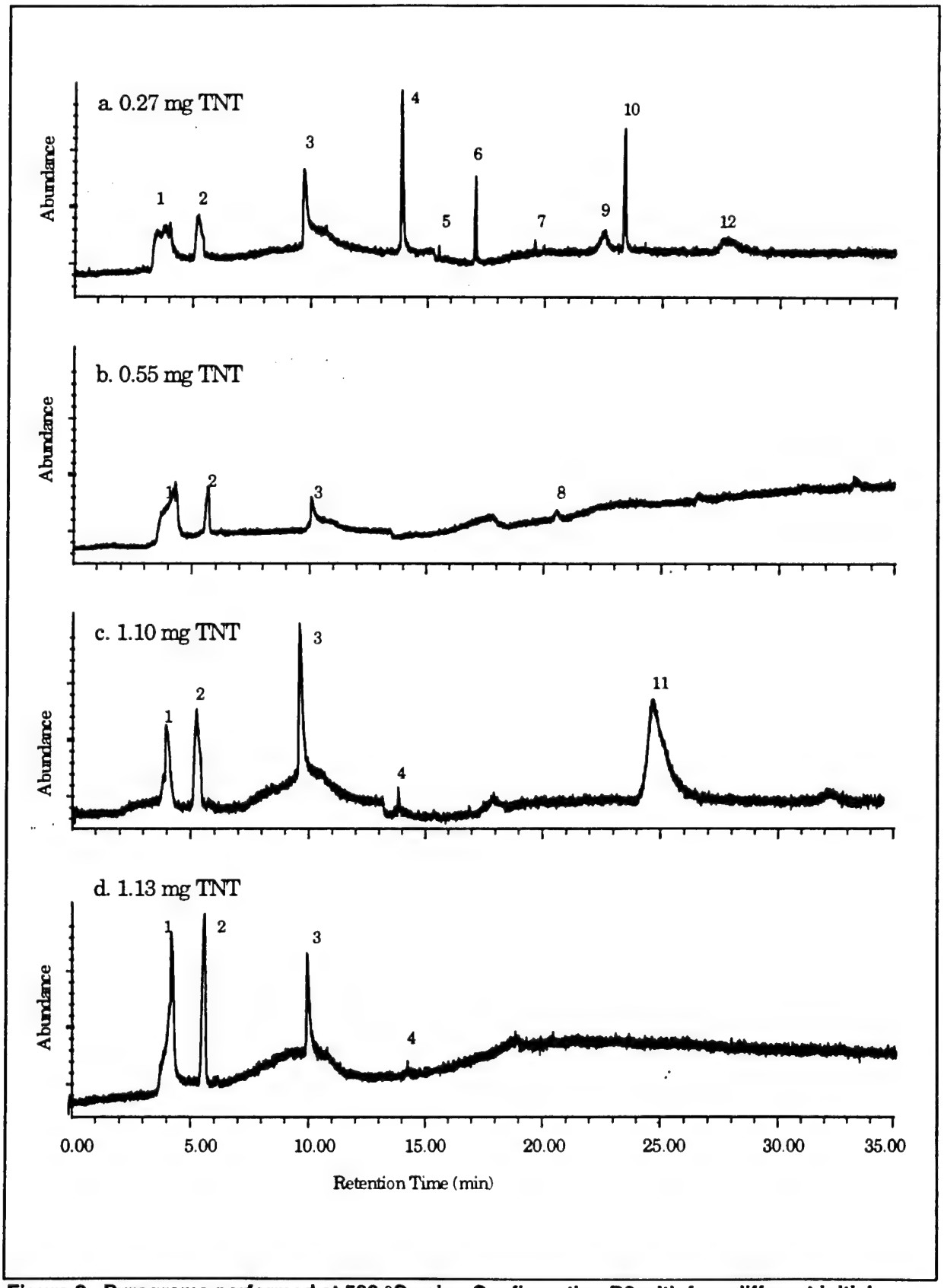

Figure 8. Pyrograms performed at 500 °C using Configuration B2 with four different initial masses of TNT.

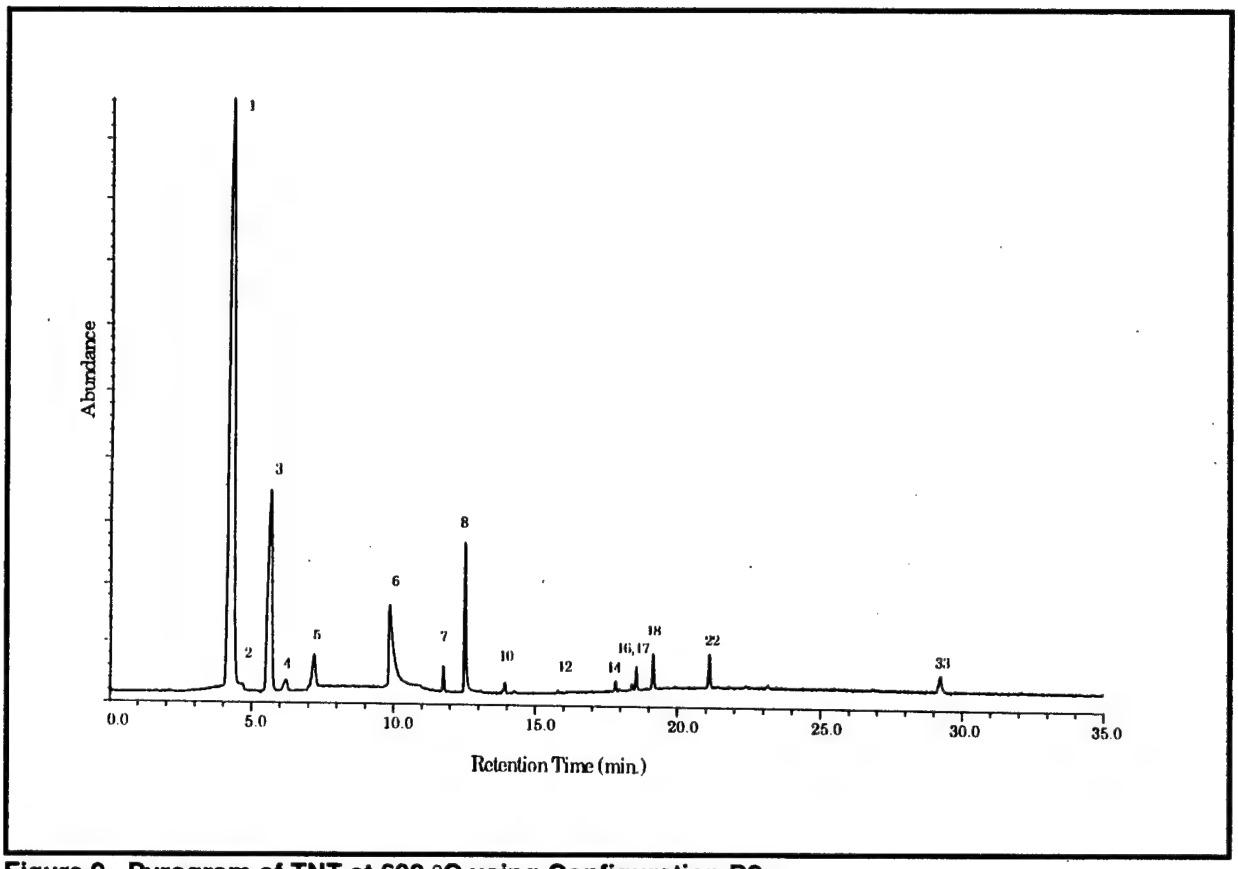

Figure 9. Pyrogram of TNT at 600 °C using Configuration B2.

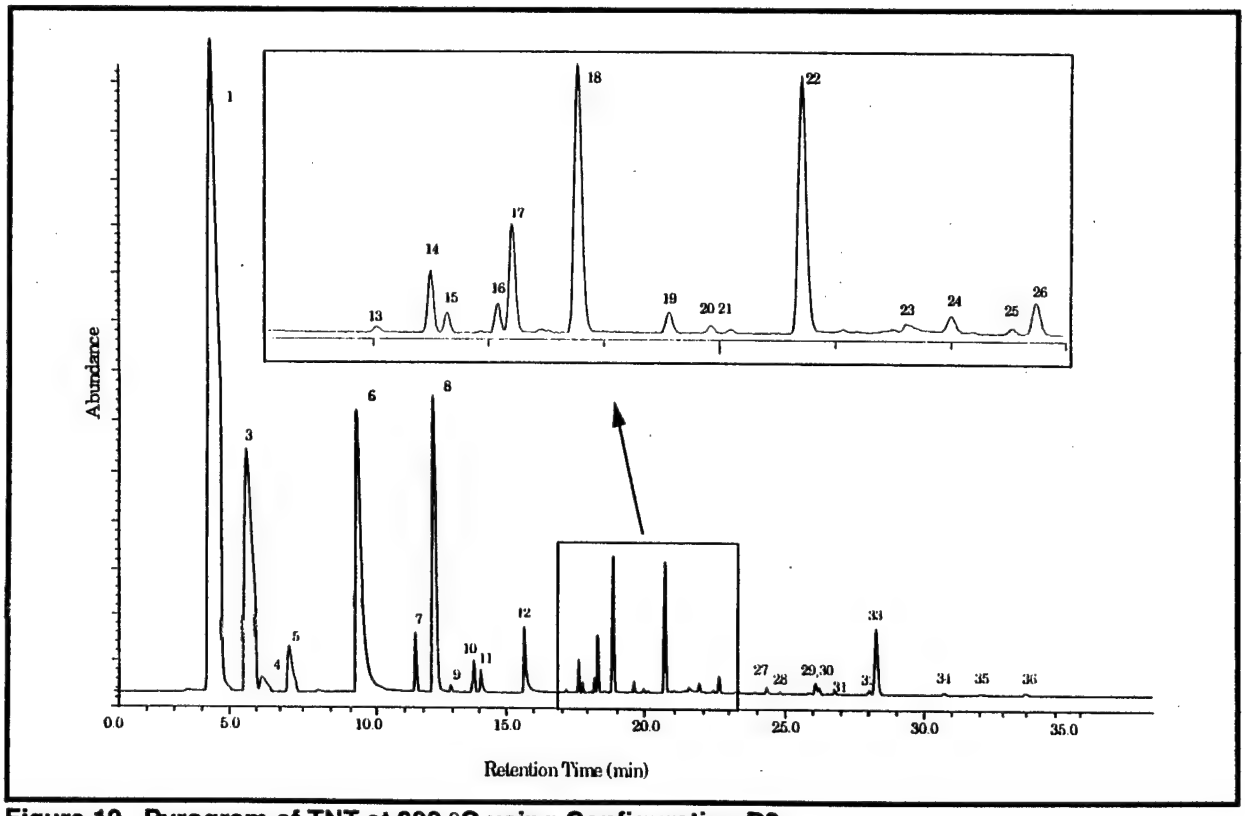

Figure 10. Pyrogram of TNT at 900 °C using Configuration B2.

Table 8. Pyrolytic by-products of TNT at 500 °C using Configuration B2.

	Experiment 8a	Experiment 8b	Experiment 8c	Experiment 8d
Fraction I				
1	N_2, O_2, CO, NO	N_2, O_2, CO, NO	N_2, CO, NO	N_2, O_2, CO, NO
2	CO_2	CO_2	CO_2	CO_2
3	H_2O	H_2O	H_2O	H_2O
Fraction II				
4	CH_3OH	—	CH_3OH	CH_3OH
5	Acetaldehyde	—	—	—
6	Methyl formate	—	—	—
7	2-Propenal	—	—	—
8	—	Toluene	—	—
9	Styrene	—	—	—
10	Unknown	—	—	—
11	—	—	Benzonitrile	—
12	Phenol	—	—	—

Figure 8a-d shows some problems with pyrolysis reproducibility. These four pyrograms all have identical pyrolytic conditions including a final set temperature of 500 °C. These four experiments differ only in the initial mass of TNT used. It is expected that the results would only differ in the peak intensities. While similar in many respects, however, the pyrograms are not completely identical. For Figure 8a-d, 0.27 mg, 0.55 mg, 1.10 mg and 1.13 mg of TNT were placed into the quartz tube, respectively. Figure 8a has the greatest number of by-products despite pyrolyzing the lowest mass of TNT. Figures 8b and 8d are similar, but Figure 8c has a large peak at 25 minutes not seen elsewhere.

Table 8 identifies the peaks for Figures 8a-d of increasing retention time. Peaks 1 through 4 are common to more than one pyrogram while peaks 5 through 12 are each present in only one of the four pyrograms. Peak 1 consists of the co-elution of four light gases, N_2, O_2, CO, and NO although Experiment 8c has no O_2. All of the four pyrograms contain CO_2 and H_2O. These peaks may be related to simply drying the TNT and removing and evacuating air pockets. Peaks 4 and 6, methanol and methyl formate, as mentioned before, are likely solvent related. These species are appreciable in Figure 8a, but methanol is small in Figures 8c and 8d, and absent in Figure 8b, indicating possible sample nonhomogeneity. Peak 5 is tentatively identified as acetaldehyde. This peak has been seen in samples of other EM. Figure 11a is the mass spectrum for peak 5 from Figure 8a. Figure 11b and 11c show the mass spectra for ethylene oxide and acetaldehyde, respectively. All three mass spectra are very similar, however, acetaldehyde is a better match for peak 5 due to the better agreement in the 42:43:44 peak ratios.

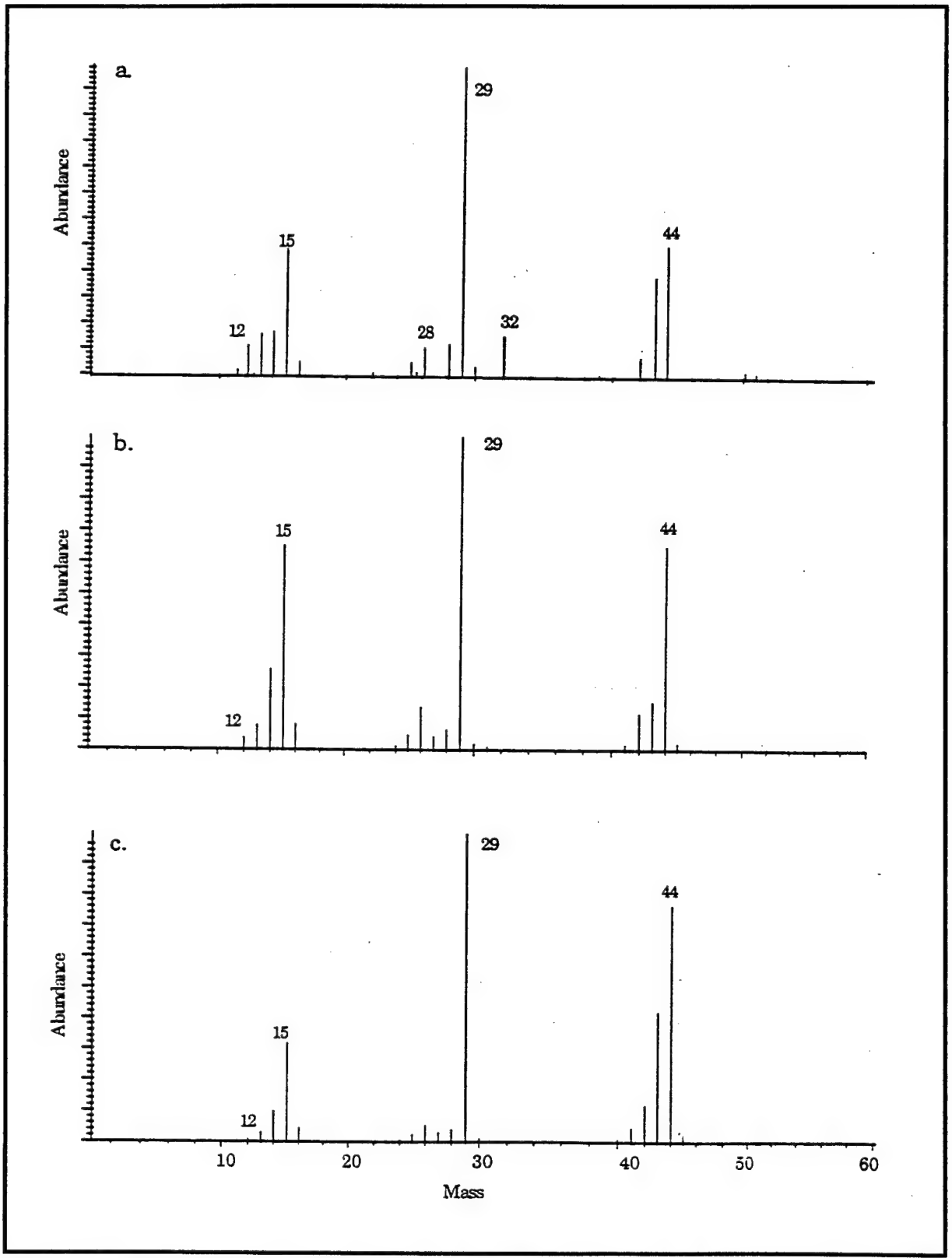

Figure 11. Mass analysis of peak 5 from the pyrogram in Figure 8a; shown are: (1) the mass spectrum of peak 5, (b) the mass spectrum of ethylene oxide, and (c) the mass spectrum of acetaldehyde.

The remaining peaks all seem plausible by-products from TNT degradation. It is interesting, however, that there are no common products above 18 minutes. Aromatics such as toluene, styrene, phenol, and benzonitrile are produced. All have the aromatic ring of TNT, a complete loss of all nitro groups and some degree of rearrangement to obtain the ring substituents. The smaller by-products are 2-propanal (peak 7) and an unknown compound (peak 10). The mass spectrum of peak 10 is seen in Figure 12a. The best library match was dimethyl ether, Figure 12b. However, when comparing the two spectra, the match is questionable. Peak 10 may have a molecular ion peak at 74 amu and lacks the 46 amu peak of dimethyl ether. It also has a non-negligible 44 amu mass peak, which is not present in the dimethyl ether mass spectrum.

The dramatic difference between the general pattern of the pyrograms at 500 °C and a pyrogram done at 600 °C (Figure 9) indicates that a temperature region exists between 500 and 600 °C where the decomposition mechanism changes from a solid phase mechanism at lower temperatures to a vapor phase mechanism at higher temperatures with concomitant high gas production. It is possible that any instability or nonreproducibility in the pyrolytic temperatures near this critical temperature region can have a large effect on by-product formation. At this point, the initial mass of the TNT may have an increased influence, with greater unreacted masses acting as adsorption sites or catalysts.

Figure 9 shows the pyrogram of 0.26 mg of TNT at 600 °C. The additional 100 °C drastically increases the degree of pyrolysis as seen by the increased abundance and variety of by-products. Figure 10 is a pyrogram of 0.39 mg of TNT at 900 °C. Interestingly, we note that as the pyrolytic temperature increases from 600 to 900 °C, the variety and the abundance of by-products increases. This behavior is opposite that of RDX, which has a decreased amount of by-products as the pyrolytic temperature increases. TNT must require a much higher temperature to reach the point when the variety and abundance of Fraction II by-products begins to decrease.

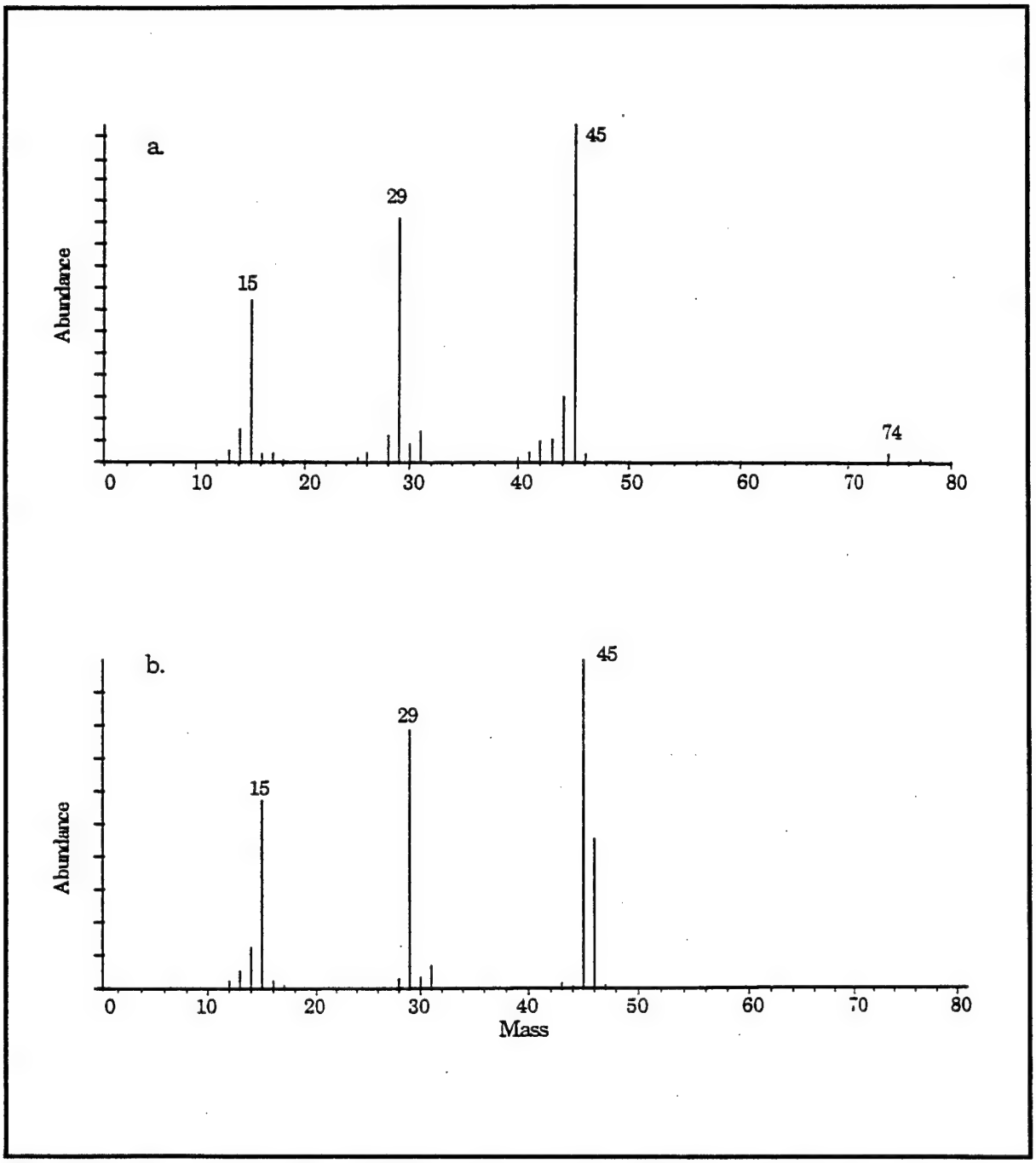

Figure 12. Mass analysis of peak 10 from the pyrogram in Figure 8a. Shown are (a) the mass spectrum of peak 10 and (b) the mass spectrum of dimethyl ether.

The numbered peaks on Figures 9 and 10 correspond to the identified by-products numbered in Table 9. Compounds marked by an "x" indicate its presence in the pyrogram for a particular temperature. Many of the light Fraction I gases are the same as those produced at 500 °C. New species are also formed such as methane, N_2O, and acetylene, which all elute before water. Also, there is no evidence of N_2 or O_2 present in peak 1 as at 500 °C.

Table 9. TNT pyrolytic by-products at 600 °C and 900 °C using Configuration B2.

Peak	Molecular Formula / Common Name	600°C	900°C
	Fraction I		
1	CO, NO	x	x
2	CH_4	x	-
3	CO_2	x	x
4	N_2O	x	x
5	HC≡CH	x	x
6	H_2O	x	x
	Fraction II		
7	$(CN)_2$	x	x
8	HCN	x	x
9	Propene	-	x
10	1,2-Propadiene	x	x
11	Methanol	-	x
12	Unknown	x	x
13	Methyl formate	-	x
14	1-Buten-3-yne	x	x
15	Unknown	x	x
16	1,3-Butadiyne	x	x
17	Propiolonitrile	x	x
18	Acetonitrile	x	x
19	2-Propenal	-	x
20	Furan	-	x
21	Acetone	-	x
22	2-Methyl-2-propenenitrile	x	x
23	Acetic acid	-	x
24	3-Penten-1-yne	-	x
25	Unknown	-	x
26	Propanenitrile	-	x
27	2-Propenenitrile	-	x
28	Unknown	-	x
29	Unknown	-	x
30	2-Butenenitrile	-	x
31	3-Butenenitrile	-	x
32	2-Butenenitrile	-	x
33	Benzene	x	x
34	Pyrrole	-	x
35	Acetamide	-	x
36	Pyridine	-	x

The Fraction II species are nearly all different from those produced at 500 °C. While most of the 500 °C by-products retain the aromatic ring structure of TNT, benzene is the only aromatic by-product resulting from 600 °C pyrolysis. HCN

is the largest Fraction II by-product and the related product $(CN)_2$ is also produced to a larger extent than with RDX.

Most of the Fraction II species are unsaturated hydrocarbons frequently containing a nitrile bond, C≡N. Nitrogroup elimination certainly occurs, e.g., benzene, but it seems unlikely that these nitro groups would then return to the ring fragments to rearrange and form the nitrile species. A more likely scenario is rearrangement of the C-NO_2 moiety to the C≡N, especially in light of the fact that the identified species only have a single C≡N bond. Multiple occurrences of C≡N would be expected if nitrogen-containing species (e.g., nitro, nitrite, and nitrate groups) attack the hydrocarbon fragments. Surprisingly, although pyrolysis of TNT results in acetaldehyde, acetic acid, and acetamide, there was no detected formaldehyde, formic acid, or formamide as seen in RDX.

The identification of peak 12 is difficult. Although it is produced only slightly at 600 °C, it is a substantial by-product at 900 °C. Figure 13 shows the mass spectrum of peak 12, which can be compared to the mass spectra of ethylene oxide and acetaldehyde presented in Figure 11b and 11c, respectively. The major 44 amu peak present in both the acetaldehyde and the ethylene oxide spectra is only a minor peak in Figure 13. Other differences include the much smaller 29 amu peak and the now dominant 43 amu peak. This leads to the conclusion that peak 12 is neither acetaldehyde nor ethylene oxide. The mass spectra of peak 12 is in fact nearly identical to the unknown species produced during pyrolysis of RDX at 500 °C (see Figure 2, peak 8).

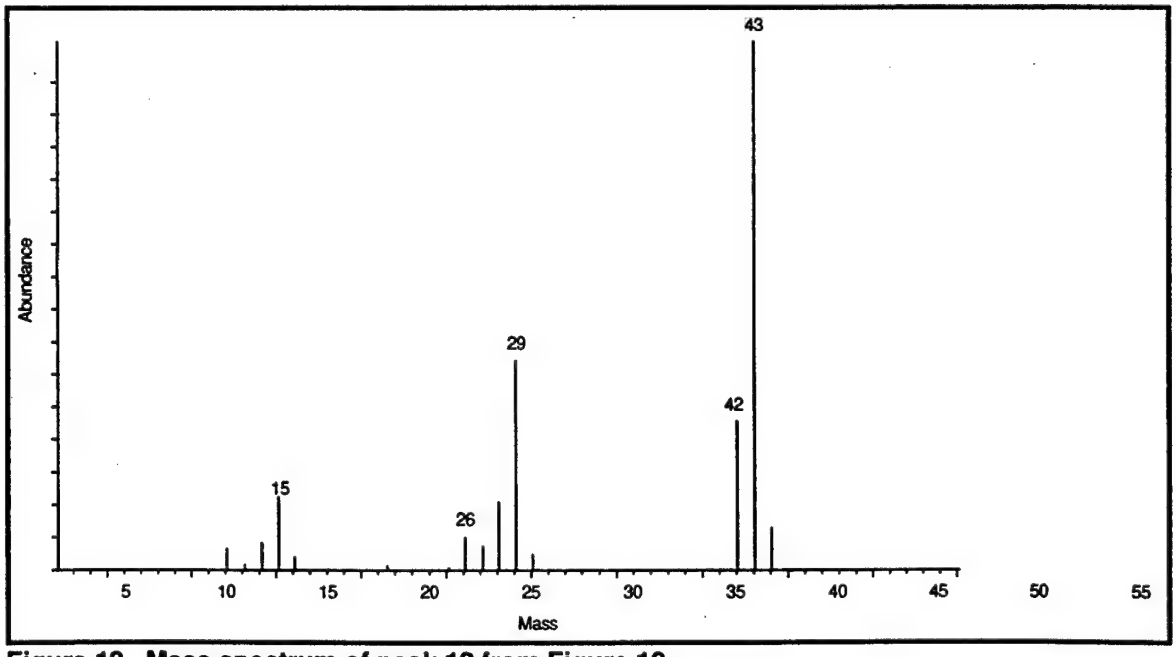

Figure 13. Mass spectrum of peak 12 from Figure 10.

Furan, pyrrole, and pyridine are three products that require the ring structure to be broken then reformed. The fact that these products are formed in increasing abundance as the pyrolytic temperature increases to 900 °C indicates that higher temperatures are needed to create these compounds and a much higher pyrolytic temperature is required to initiate further breakdown of by-products than that needed by RDX.

The MS library provided no suitable matches for peaks 15, 25, 28, and 29. The MS for these four peaks, in ascending numerical order, are shown in Figure 14a-d. These peaks are quite small; better results will require pyrolysis of a greater mass of TNT and perhaps a different pyrolysis temperature to maximize production of these by-products. The list of compounds in Table 9 that do provide good library matches indicates that these unknown compounds may be unsaturated hydrocarbons with a nitrile bond.

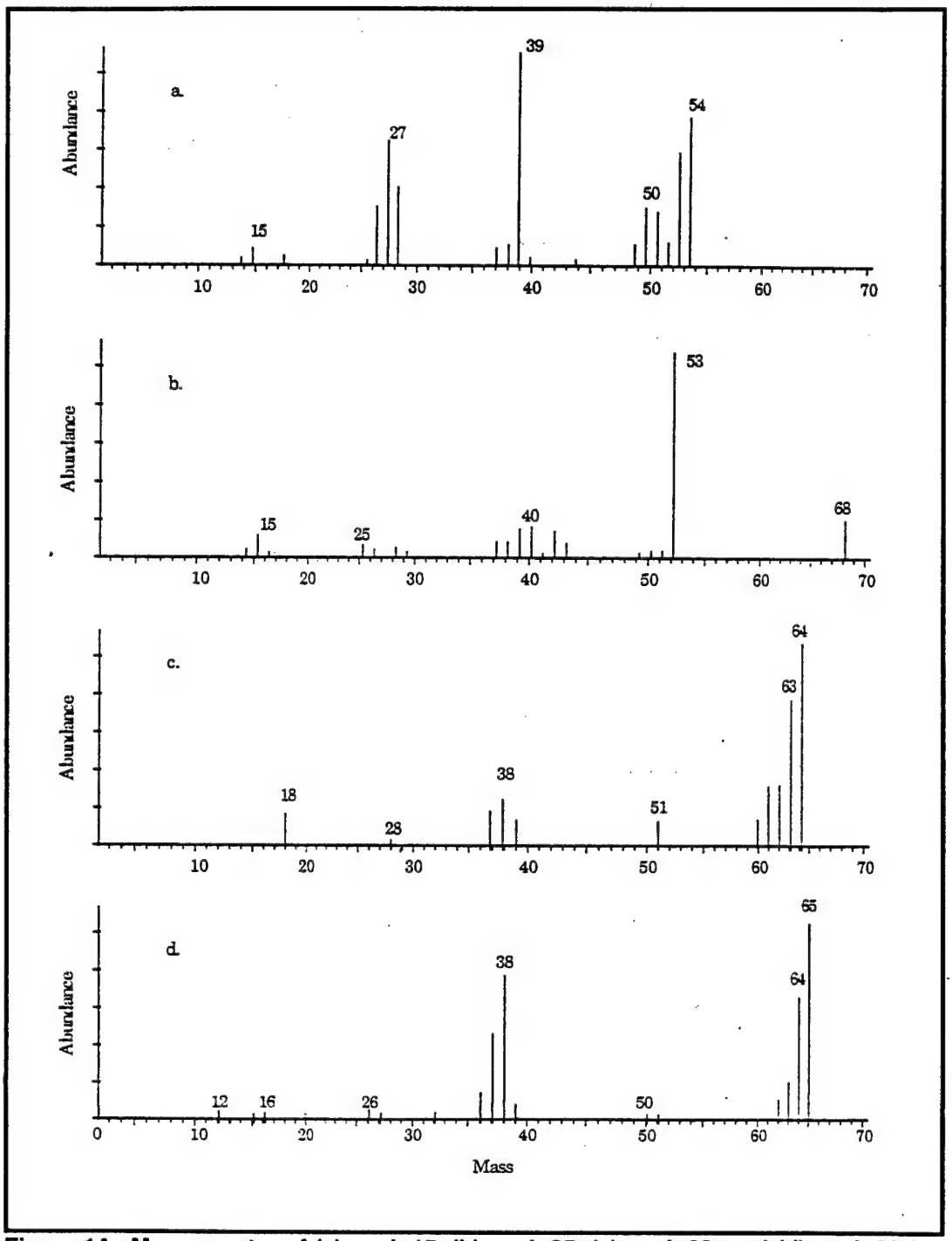

Figure 14. Mass spectra of (a) peak 15, (b) peak 25, (c) peak 28, and (d) peak 29 from Figure 10.

5 Pentaerythritol Tetranitrate (PETN)

Background

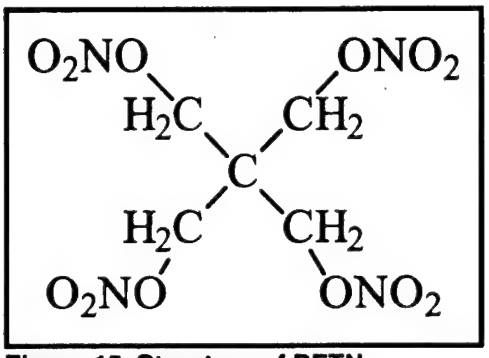

Figure 15. Structure of PETN.

Pentaerythritol tetranitrate (PETN) belongs to the nitrate ester class of energetics. The structure of PETN (Figure 15), is highly symmetric with four nitrate ester groups bonded to a central carbon atom. PETN (MW = 316.2) melts at 141.5 °C, and explodes between 205 and 225 °C. At room temperature, PETN is insoluble in water (0.2 mg / 100 g), but soluble in ethyl acetate (6.3 g / 100 g) and acetone (20.3 g / 100 g). PETN is employed as a second base charge in blasting caps and detonators, as a booster charge, and in detonation cords, since PETN displays a higher stability and sensitivity relative to other energetics (Bailey and Murray 1984). Also, PETN is relatively nontoxic to humans and the environment presumably because of its low solubility in water (Yinon and Zitrin 1993).

Table 10 lists the various reported decomposition products of PETN. Differences in reported by-products are due to differences in experiment goals, temperatures of decomposition, and the instrumentation. The major characteristic that stands out on this list of by-products is the small number of Fraction II compounds. Only HCN, CH_2O, CH_3ONO and CH_3ONO_2 have been previously observed. Not all of the products listed in Table 10 are due to pyrolytic breakdown of PETN. By-products attributed to Blais and co-workers (Blais, Greiner, and Fernandez 1990), result from detonation of PETN while the observed methyl nitrite (CH_3ONO) (Field et al. 1985) is due to fracture induced decomposition. PETN decomposition initiated by low and high energy laser pulses has also been examined (Field et al. 1985).

Results

PETN was pyrolyzed using Configuration A2 under several different conditions. However, little peak identification was reported. Therefore, conclusions from this data were based solely on trends in the pyrogram patterns. Three different operational parameters were examined: the effect of the pyrolysis temperature, the effect of the heating ramp rate, and the effect of the pyrolysis holding time.

Table 10. Reference list of previously observed by-products from the pyrolysis of PETN.

Molecular Formula	Molecular Weight	Reference
H_2	2	1
H_2O	18	2,3,4
C_2H_2	26	2
HCN	27	2,4
N_2	28	1,3
CO	28	1,2,3
CH_2O	29	1,2,3
NO	30	1,2,3
N_2O	44	3
CO_2	44	1,2,3
NO_2	46	1,2,3
CH_3ONO	61	5
CH_3ONO_2	77	3
HNO*	31	3
CH_3OH*	32	3
HONO*	47	3

[1] Roth 1949
[2] Oyumi and Brill 1986b
[3] Ng, Field, and Hauser 1976
[4] Blais, Greiner, and Fernandez 1990
[5] Field et al. 1985
* Species proposed but not observed.

Figure 16a-d shows pyrograms resulting from the pyrolysis temperatures of 300, 500, 700, and 900 °C, respectively, all with a ramp rate of 20 °C/msec and a hold time of 2 seconds. It is expected that as the temperature increases, the amounts and variety of Fraction II compounds would decrease due to greater sample and by-product decomposition. This conclusion is not readily apparent from Figure 16 as the pyrograms appear remarkably similar. The primary difference is the presence of a peak (scan 800) on the shoulder of the large CO_2 peak that is small at 300 °C, grows at 500 and 700 °C, and disappears at 900 °C. There may possibly be more species present between scans 3000-4500 at 300 °C than at 900 °C, but there is not a substantial difference. Note that all four pyrolytic temperatures are above the PETN decomposition temperature. Thus, the pyrolytic decomposition mechanism of PETN is relatively insensitive above its decomposition temperature. This behavior is unlike that of RDX and TNT, where the by-products change significantly at different temperatures above the decomposition temperature.

Figure 17a-d shows the effect of the pyrolytic heating ramp rate on the by-products from PETN at a final temperature of 300 °C and a 2 second holding time. Heating ramp rates of 0.2, 2.0, and 20 °C/msec are used in Figure 17b-d, respectively. There is little effect on the PETN by-products due to any thermal shock at the higher ramp rate. Figure 17a shows a heating ramp of 0.08 °C/msec. Clearly, the pyrogram is substantially different than the previous three. This behavior illustrates a problem with the older Model 100 Pyroprobe systems. The holding time begins immediately on the start signal. If the heating ramp rate is too slow, the system may not attain the desired pyrolysis temperature before the end of the holding time.

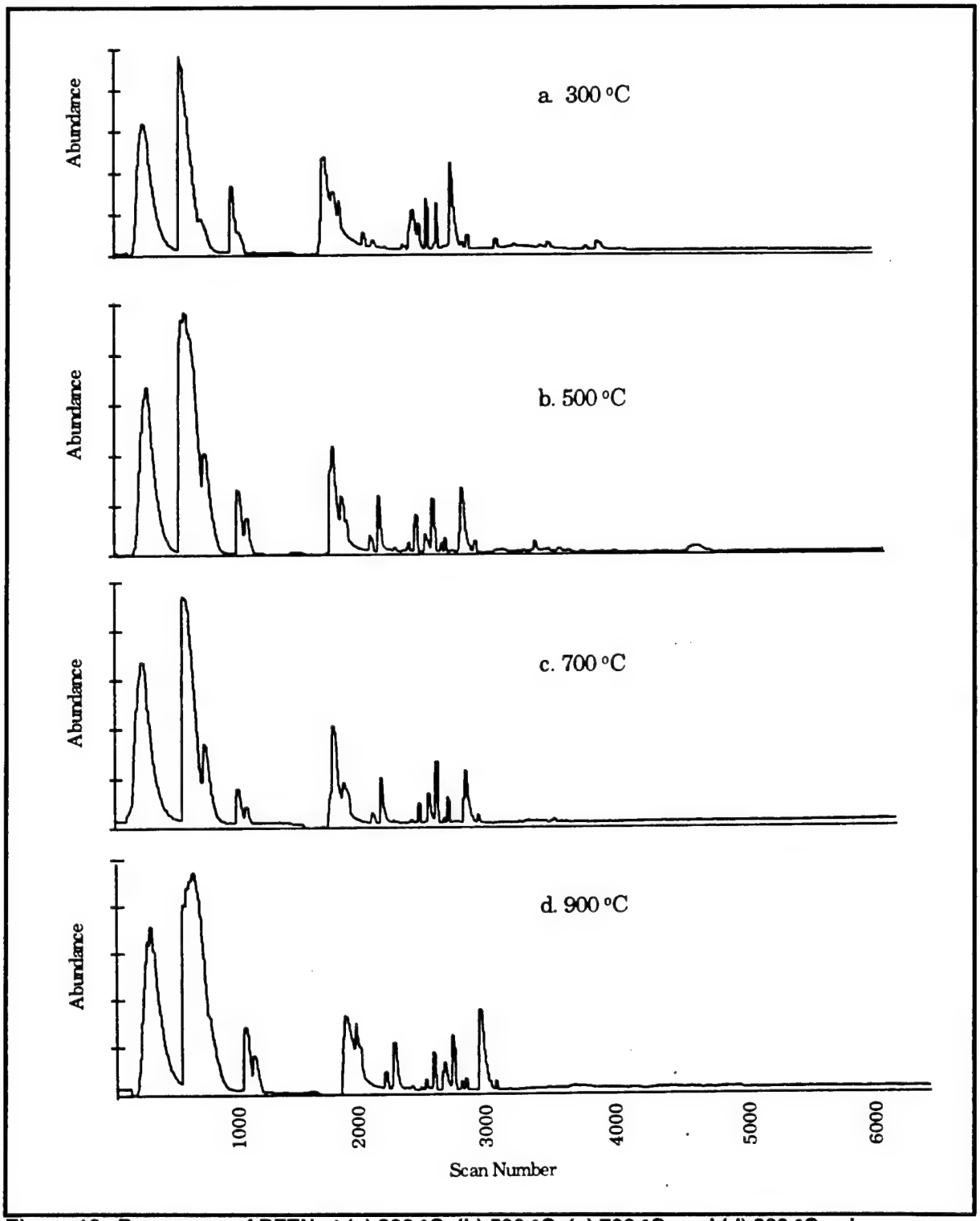

Figure 16. Pyrograms of PETN at (a) 300 °C, (b) 500 °C, (c) 700 °C, and (d) 900 °C using Configuration A2.

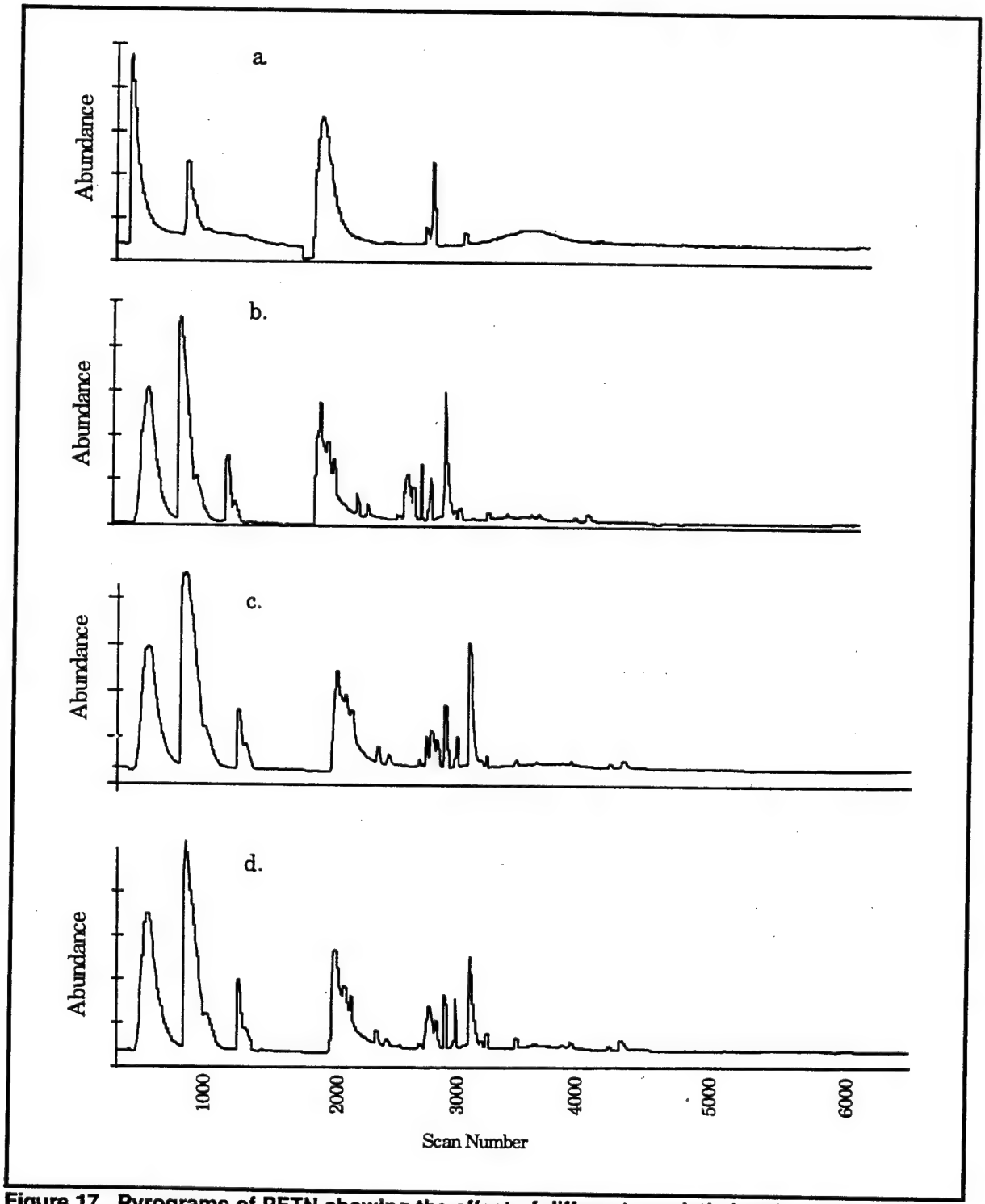

Figure 17. Pyrograms of PETN showing the effect of different pyrolytic heating ramp rates with a final temperature of 300 °C and a 2 second holding time. Shown are a ramp rate of (a) 0.08 °C/msec, (b) 0.2 °C/msec, (c) 2.0 °C/msec, and (d) 20.0 °C/msec.

The pyroprobe electronics assumes that the heating element starts at 0 °C and begins supplying current in accordance with this assumption. In the particular case of Figure 17a, the following calculation shows that the heating element only reaches 160 °C.

$$0.08\,^{\circ}C/\mathrm{msec} \times 2.0\,\mathrm{sec} \times 1000\,\mathrm{msec/sec} = 160\,^{\circ}C$$

This temperature is well below the ignition temperature and thus it is not surprising that fewer peaks are seen. These peaks may be due to drying and purging the PETN sample rather than to any pyrolytic mechanism.

Figure 18a-c shows the effect of the pyrolytic hold time. The final pyrolysis temperature of 300 °C and the ramp rate of 20 °C/msec are constant, but the different holding times are 0.02, 0.1, and 2.0 seconds in Figure 18a through c, respectively. The same problem is noted here as in Figure 17a. Using the same equation shown previously, one can calculate the amount of time that the heating element is maintained at the desired temperature. With a 0.02 second holding time, the platinum coil reaches 300 °C in 15 msec and it is held at this temperature for 5 msec (20 - 15 msec). Based on the pyrogram of Figure 18a, this time is not long enough to effect any pyrolysis of PETN and, due to the thermal resistivity of the quartz, the sample likely does not experience the 300 °C pyrolysis temperature. The sample is only heated enough to drive off acetone (a possible solvent), and entrained water. The next longer holding time, 0.1 sec, results in an 85 msec time period at 300 °C. Surprisingly, this is still not enough time to completely pyrolyze the sample. The appearance of the initial peaks at scan 200 and 680 indicate some breakdown is occurring to produce light gases. The two small peaks bounding the large acetone peak are two small Fraction II by-products from either PETN or acetone. Figure 18c shows the effect of a longer hold time at 300 °C or 985 msec (1000 msec - 15 msec). This pyrogram is equivalent to those in Figure 16, indicating the complete pyrolytic breakdown of PETN. This experiment clearly shows the need for care in the choice of the pyrolytic hold time.

Figure 19 shows a pyrogram done at 300 °C using Configuration B3. This data is shown primarily to help identify the peaks observed in the previous figures. Excess sample is indicated by the poor peak shape and low resolution. The peak identification for the numbered peaks is given in Table 11. The separate peak (peak 1) for co-eluting nitrogen and oxygen has not been previously observed. Appreciable quantities of N_2O and ethylene are observed, unlike TNT and RDX pyrolysis.

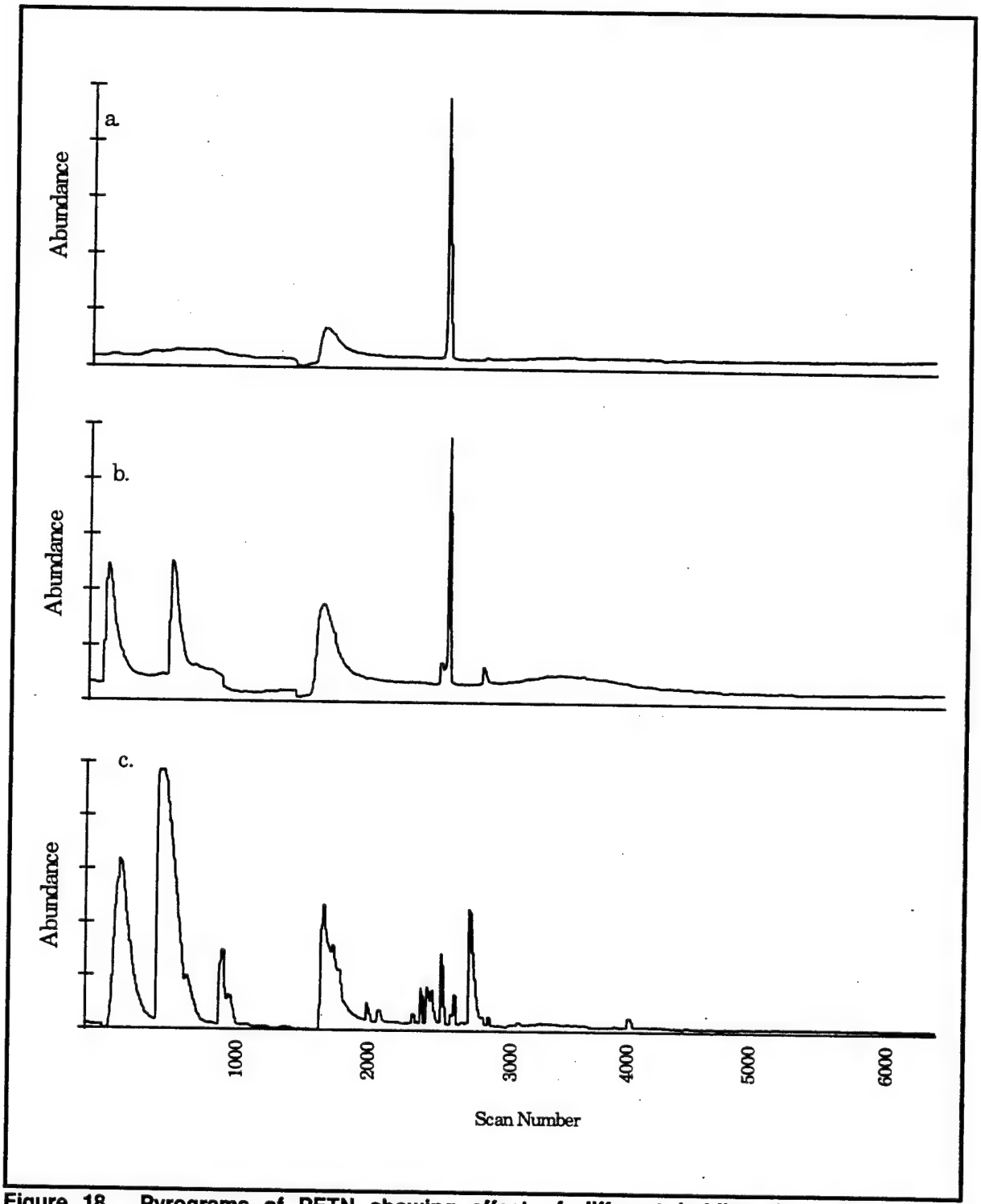

Figure 18. Pyrograms of PETN showing effect of different holding times with a final temperature of 300 °C and a heating ramp rate of 20 °C/msec. Shown are holding times of (a) 0.02, (b) 0.1, and (c) 2.0 seconds.

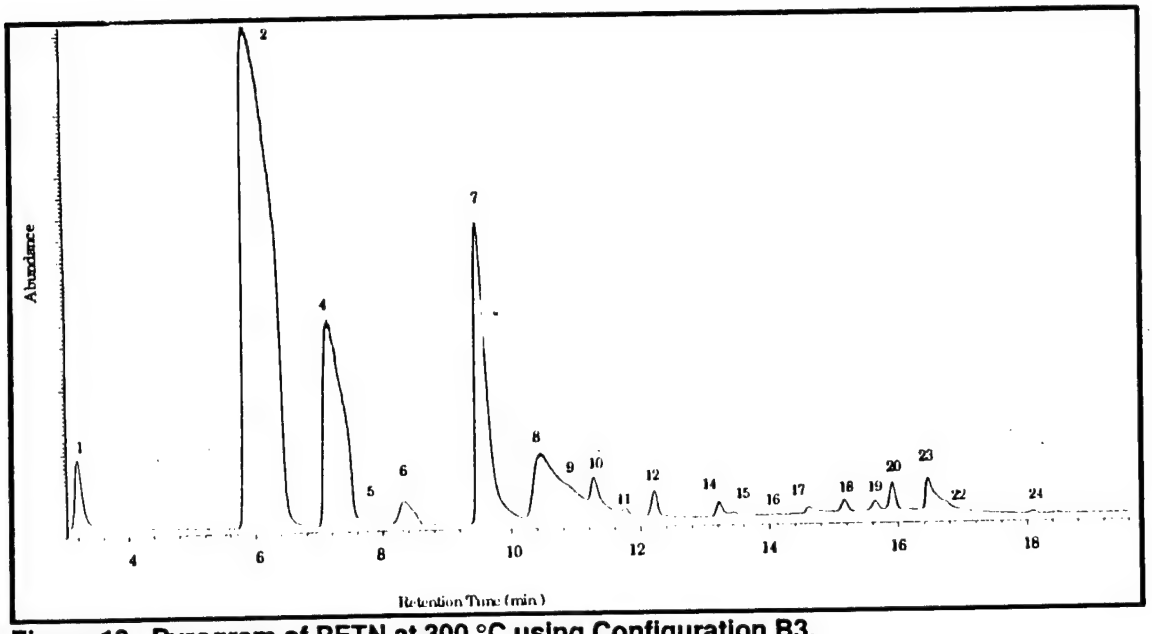

Figure 19. Pyrogram of PETN at 300 °C using Configuration B3.

Table 11. Pyrolytic by-products from PETN at 300 °C and 900 °C using Configuration B3.

Peak #	Molecular Formula / Common Name	300 °C	900 °C
Fraction I			
1	N_2 / O_2	x	
2	NO /CO	x	x
3	CH_4		x
4	CO_2	x	x
5	N_2O	x	x
6	C_2H_4	x	x
7	H_2O	x	x
Fraction II			
8	HCHO	x	x
9	$(CN)_2$	x	
10	HCN	x	x
11	C_3H_6	x	x
12	1,2-Propadiene	x	x
13	Propyne		x
14	Ethylene oxide or Acetaldehyde	x	x
15	Ethylene oxide or Acetaldehyde	x	x
16	Methyl formate	x	x
17	Formic acid	x	
18	Acetonitrile	x	x
19	2-Propenal	x	x
20	Acetone	x	x
21	2-Propenenitrile		x
22	Nitromethane	x	x
23	Acetic acid	x	x
24	2-Butenal	x	x

Since the PETN was not vacuum dried before use, it is surmised that acetone is present as a processing solvent, especially in light of results from Figure 18a. Therefore, several possibilities exist as an origin for by-products. The primary source is PETN decomposition, but acetone decomposition and possible interaction among by-products may lead to the rich pyrogram of Figure 19. Pyrolysis of PETN accomplished in this work results in a great deal more information than previous studies. Unlike TNT, only a few Fraction II by-products contain nitrogen: $(CN)_2$ (peak 9), HCN (peak 10), and acetonitrile (peak 18).

Since the longest carbon chain in PETN is three atoms (see Figure 15), it is not surprising that none of the by-products have a chain length of more than three carbon atoms. An exception is 2-butenal (peak 24), but this peak is quite small. Table 11 also shows that the aldehyde series, formaldehyde, acetaldehyde, 2-propenal, and 2-butenal is present. A final comment is that PETN by-products are all identifiable. TNT and RDX both produce unknown ring fragments.

Figure 20 shows a pyrogram of PETN, done at 900 °C using Configuration B3. This pyrogram has superior resolution to previous runs, which may be related to a smaller PETN sample size. Table 11 also lists the identification of the numbered peaks in Figure 20. Methane (peak 3) is a new peak present among the Fraction I species. It may be present at 300 °C, but the broad NO/CO peak (peak 2) would completely obscure it.

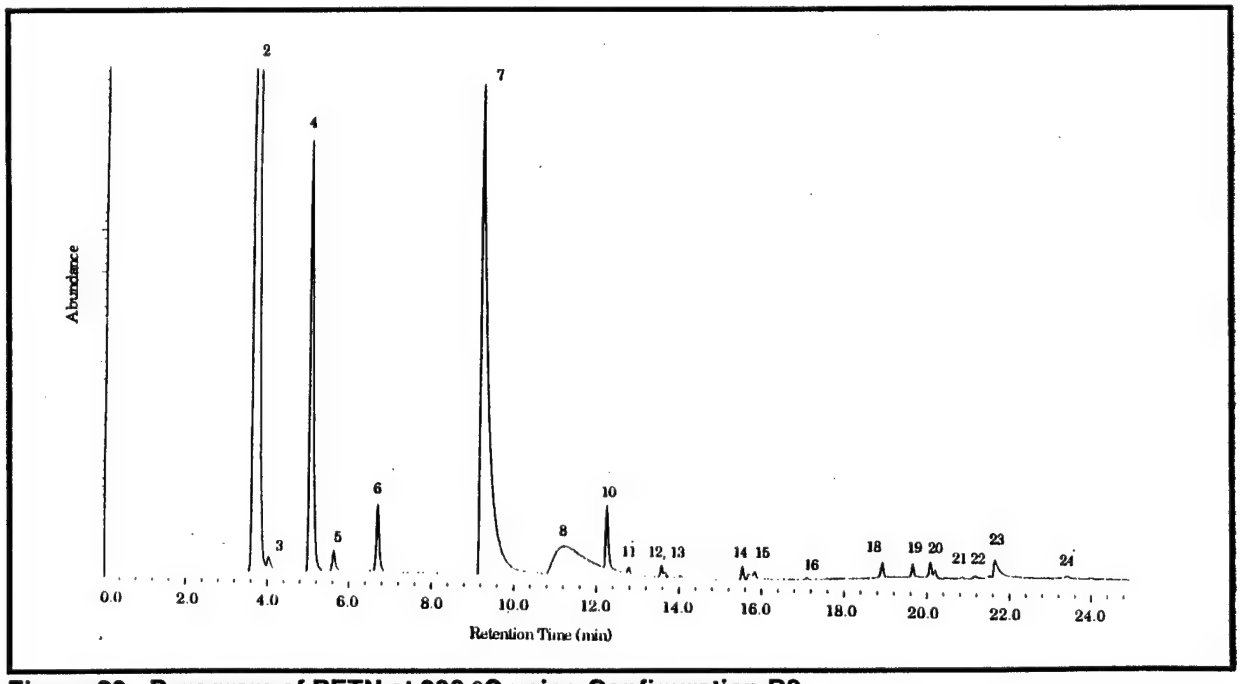

Figure 20. Pyrogram of PETN at 900 °C using Configuration B3.

Formaldehyde (peak 8) is again the dominant Fraction II species, eluting as a very broad feature. HCN (peak 10) is present, but $(CN)_2$ is not. Propene (peak 11), 1,2-propadiene (12), and propyne (13) are formed, but not propane. These compounds are all unsaturated, three-carbon molecules, as expected for PETN. Peaks 14 and 15 are separated by 0.32 min, but both have similar mass spectra, and are labeled as either ethylene oxide or acetaldehyde. Formic acid (peak 17 in Figure 19) is not observed at 900 °C; 2-propenenitrile (peak 21 in Figure 20) although very small, is not produced at 300 °C. All remaining peaks are similar to those seen during pyrolysis of PETN at 300 °C. Nitromethane is tentatively assigned as the identification of peak 22. This is the first instance noted in this report of breaking the O-NO_2 bond and reforming a by-product that retains the nitro group.

By changing the GC column, the analysis can target different compounds. Figure 21 shows the pyrogram obtained by pyrolyzing PETN at a temperature of 900 °C using Configuration B1. Any light gases that are created are not appreciably retained and elute before the 5-minute starting time shown on the figure. Unfortunately, since the peaks in Figure 21 are rather small and the molecular species are not likely present in the MS libraries, these by-products are not identified here. The two largest peaks, peak 1 at 10.3 minutes and peak 2 at 12.0 minutes, have similar mass spectra. Figure 22a shows the mass spectrum for peak 1 and Figure 22b shows the mass spectrum for peak 2. A library search of both mass spectra resulted in the common hit shown in Figure 22c, 2-methyl-2-nitro-1,3-propanediol dinitrate. The structure of this molecule, shown in the inset of Figure 22c, is very similar to PETN. This compound behaves like PETN in that it does not produce a molecular weight peak during electron ionization, but breaks down completely to produce only distinctive fragments. The NO fragment at m/z = 30, the NO_2 fragment at m/z = 46, and the CH_2-O-NO_2 fragment at m/z = 76 are common to all three spectra. This leads to the conclusion that these two high molecular weight by-products are nitrate esters with structures closely related to the structure of PETN.

After observation of both the low and high molecular weight gaseous by-products that evolve during pyrolysis, the only missing fraction is the solid residue left in the quartz tube after pyrolysis. Analysis of the residue components can serve to explain decomposition mechanisms. After pyrolysis of PETN at 900 °C, the quartz tube is removed and washed with 3 ml of ether. Figure 23 shows the chromatogram of the ether soluble components present in the residue using the HP 5MS column. Identification difficulties again lie with the small abundances of the components and the distinct possibility that the compound is not in the MS library.

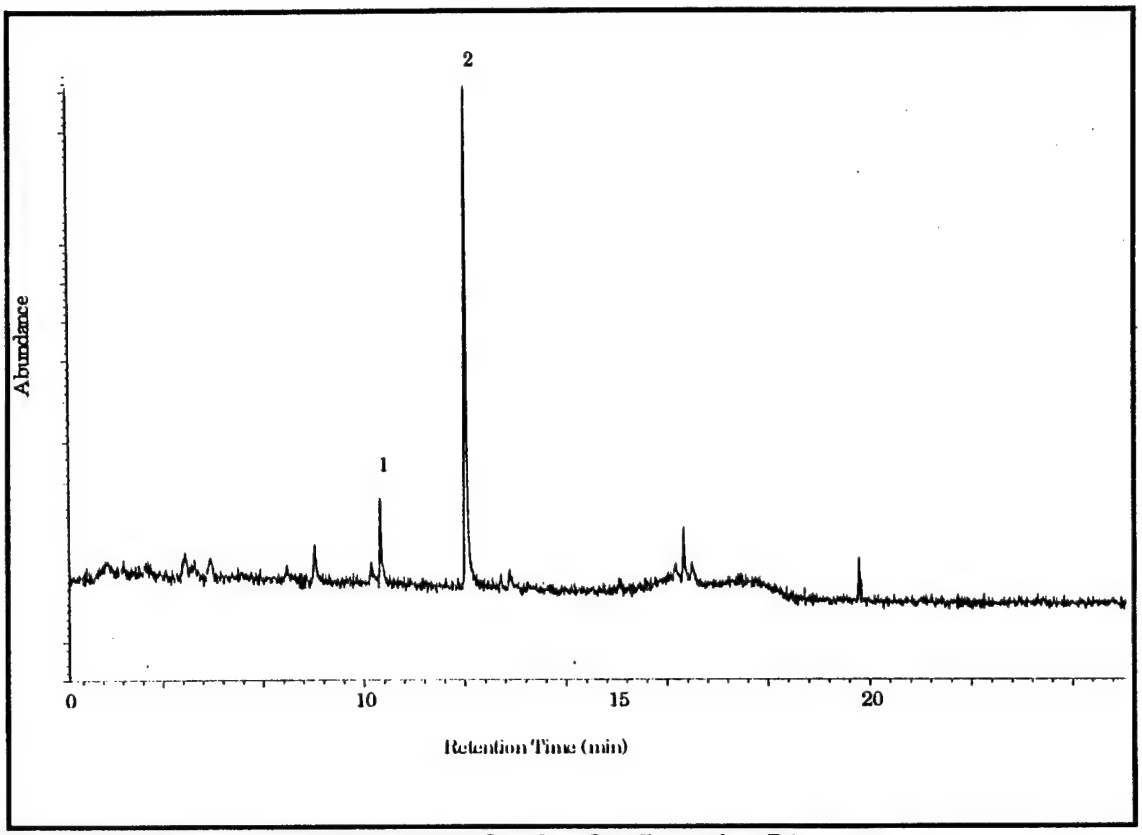

Figure 21. Pyrogram of PETN at 900 °C using Configuration B1.

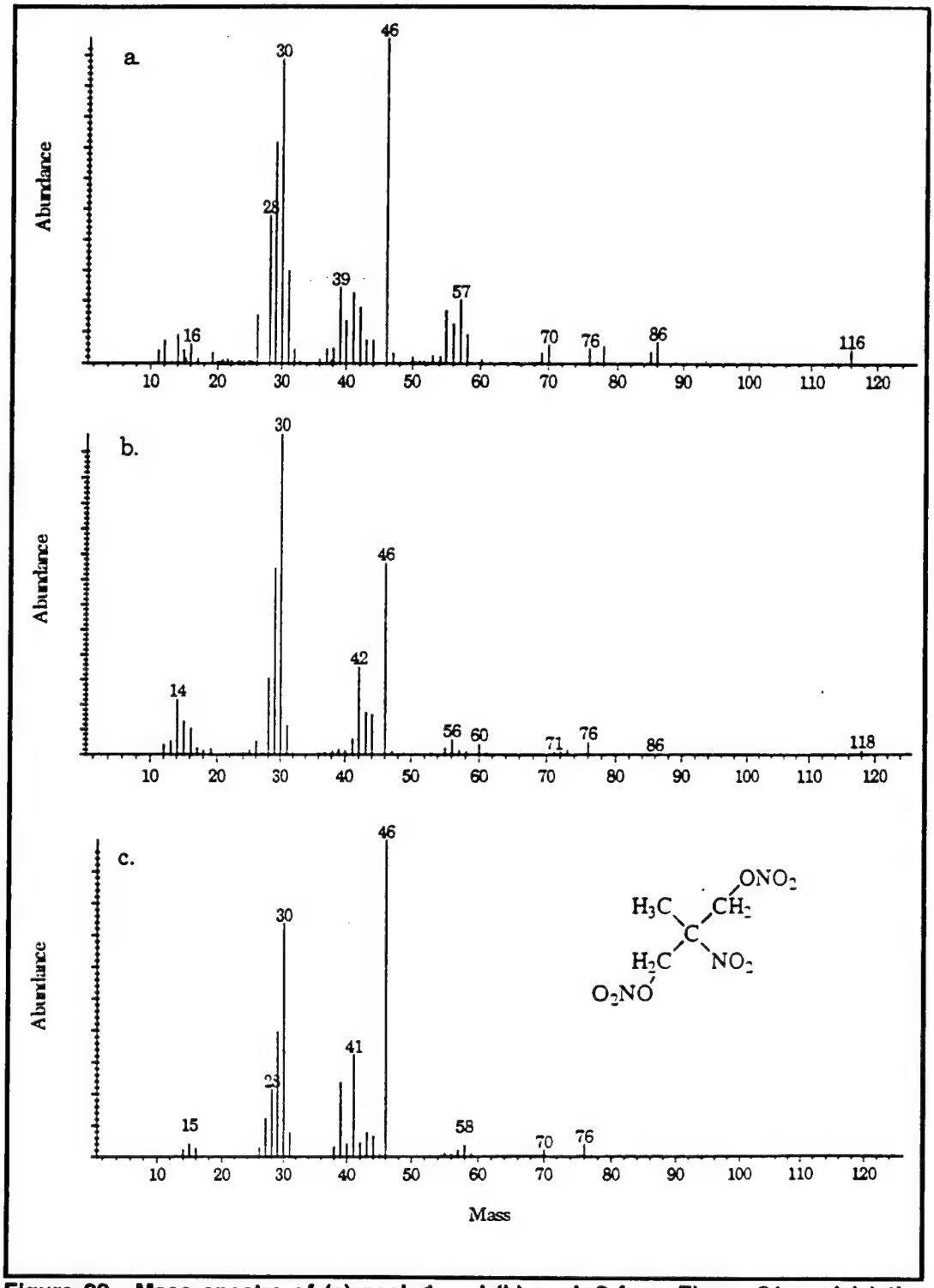

Figure 22. Mass spectra of (a) peak 1 and (b) peak 2 from Figure 21, and (c) the mass spectrum and chemical structure of 2-methyl-2-nitro-1,3-propanediol dinitrate.

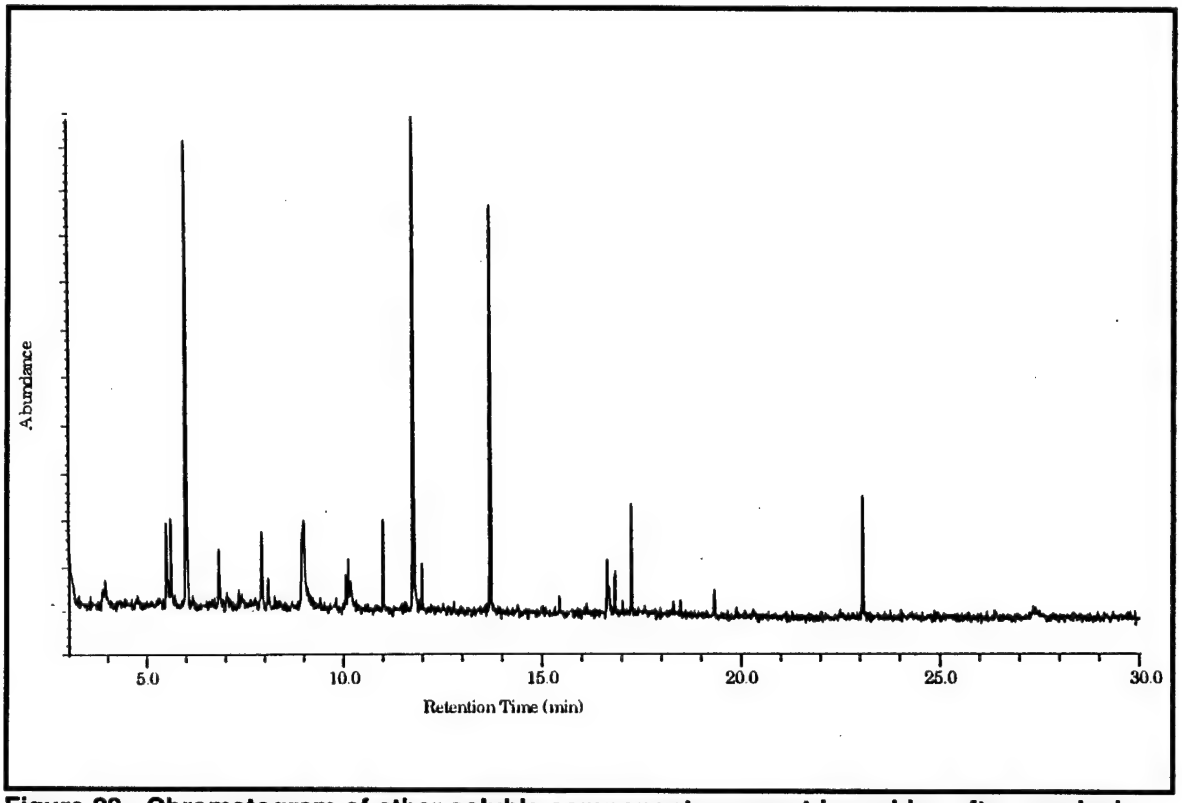

Figure 23. Chromatogram of ether soluble components present in residue after pyrolysis of PETN at 900 °C.

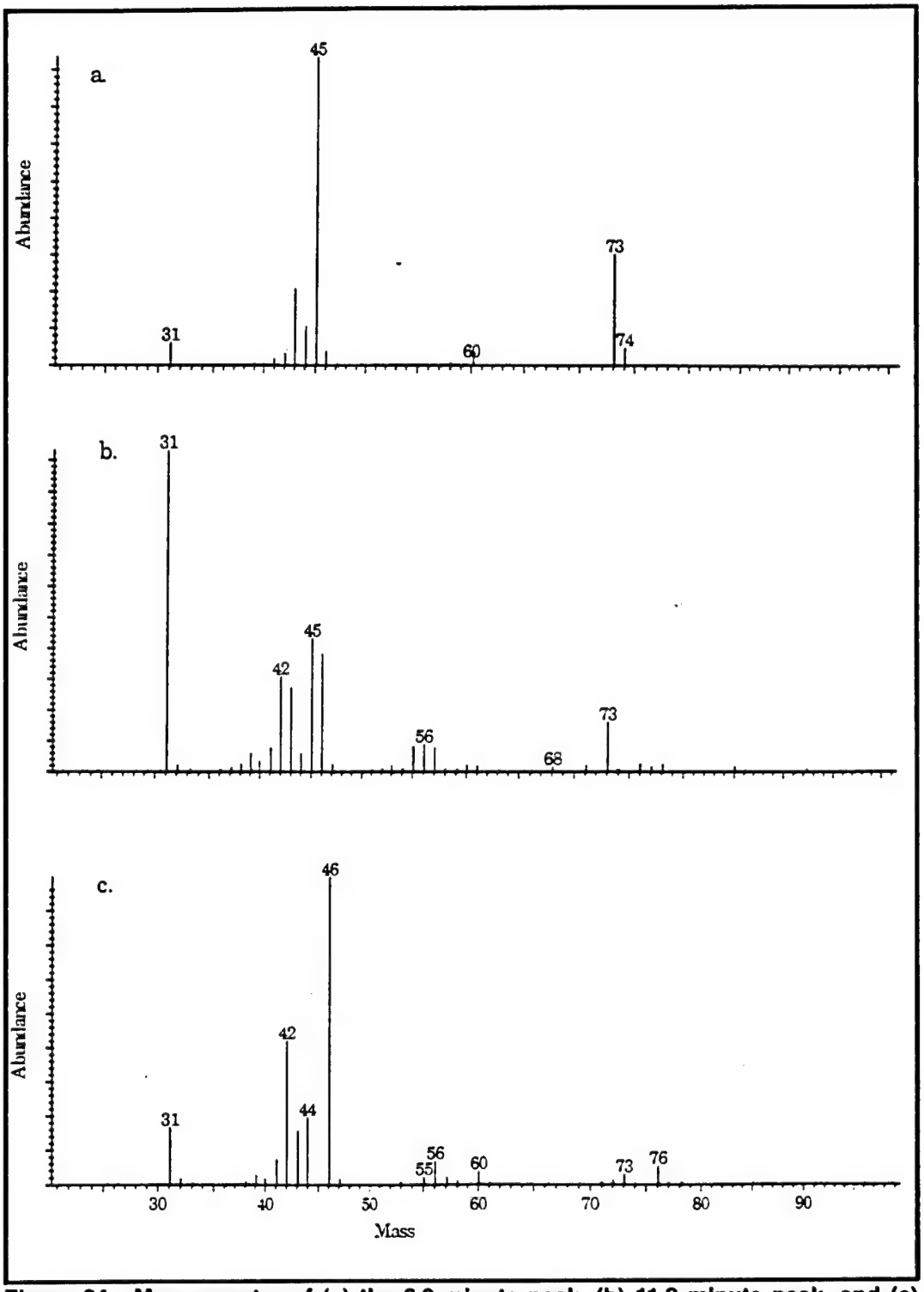

Figure 24. Mass spectra of (a) the 6.0 minute peak, (b) 11.8 minute peak, and (c) 13.7 minute peak from Figure 23.

Clearly, the PETN decomposition by-products have not completely finished reacting after 10 seconds at 900 °C, since numerous species remain in the residue. Most of these peaks are too small and were not identified. There are three major peaks at 6.0 minutes, 11.8 minutes, and 13.7 minutes. Figure 24 shows the mass spectra for these three peaks. None of these spectra had a reasonable library match. The mass spectrum of the 6.0 minute peak in Figure 24a indicates the presence of an ethoxy group (OCH_2CH_3, 45 amu) while the mass spectrum of the 11.8 min peak in Figure 24b shows evidence for both ethoxy and methoxy groups (OCH_3, 31 amu). These two by-products both have a peak at m/z = 73 and a lack of other major fragments, leading to the conclusion that they are somewhat similar in structure. Figure 24c shows the mass spectrum for the 13.7 min peak that has the familiar NO_2 fragment (46 amu), but, surprisingly, there is no 30 amu peak due to NO. The library search led to a hit with 2-nitro-2-[(nitroxy)methyl]-1,3-propanediol dinitrate or $O_2N\text{-}C(CH_2\text{-}O\text{-}NO_2)_3$, which is an intermediate structure between the compound shown in the inset of Figure 22c and the structure of PETN. Note the m/z = 76 fragment characteristic of the $CH_2\text{-}O\text{-}NO_2$ component of this molecule. The presence of these two by-products indicates a possible stepwise decomposition mechanism that works on one "arm" of PETN at a time.

6 Conclusions and Recommendations

Conclusions

Pyrolytic by-products were collected and identified from the thermal decomposition of three different energetic materials: RDX, TNT, and PETN. The results obtained in this study were compared to previous data. Past work on these three EM illustrate three distinct behaviors and can be summarized as follows: RDX produces a wide variety of both Fraction I and Fraction II by-products, including ring fragments and nitroso-RDX as the heaviest by-product. TNT is marked by a distinct lack of Fraction I light gases while all the Fraction II species exist in the solid phase. TNT also displays the unusual behavior of producing species that are larger than itself by the combination of radical species. PETN produces a rich number of Fraction I light gases, but very few Fraction II compounds.

These materials can be compared in terms of the relative amount of Fraction I gases produced at the expense of Fraction II products. A quick comparison of Table 2 for RDX (p 15), Table 6 for TNT (p 28), and Table 10 for PETN (p 42) shows that PETN produces the most Fraction I species at the expense of Fraction II species followed by RDX and finally TNT. Interestingly, this order, PETN > RDX > TNT, is also the order of these EM in terms of the ability to detonate and the heat of detonation (Urbanski 1964a, 1964b, 1964c).

Typically, pyrograms obtained in the USACERL laboratory were richer in content than previous work in this area. Pyrolysis of RDX duplicated many of the species from Table 2, but also produced several new compounds. Thermal degradation of TNT also created Fraction II compounds that have not been observed, most notably a plethora of species containing nitrile bonds. The solid phase was not examined after TNT decomposition, which would likely locate many of the higher molecular weight items from Table 6. PETN is another example where the by-products uncovered here were far more varied than those from past work.

Recommendations

Analysis of data from these experiments has provided many ideas regarding areas that must be studied more completely to understand the pyrolysis mechanism:

1. *Vacuum Dry and Purify the EM Before Pyrolysis.* Observations of the many pyrolytic species that have not been seen before leads quickly to the possibility of contamination. If this is the case, it is likely due to solvents that can be substantially removed under vacuum. Contamination by nonvolatile compounds is not probable since similar pyrolytic results were obtained with different batches of the same EM. Investigation of contaminant presence is clearly a priority.

2. *Use of the Newly Acquired Capability Of GC/MS/MS With Chemical Ionization.* Pyrograms performed using the HP5MS column for analysis of the higher boiling point by-products have not provided a great deal of information. This is primarily for two reasons: (1) the concentrations are small and (2) these by-products are not stable during electron ionization. Use of the new Varian Saturn 2000 may alleviate these problems. First, a larger mass of EM can be pyrolyzed to increase the concentration of the higher molecular weight fraction. Second, chemical ionization will be used to prevent the breakdown of fragile compounds and help obtain molecular weight information. Third, MS/MS analysis on the unknowns will elucidate chemical structure. Fourth, pyrolysis at lower temperatures prevents the pyrolytic breakdown of the larger species. Data shown for RDX and especially PETN illustrate many peaks that could benefit from further analysis in this fashion. Since neither of these EM make it through the electron ionization process intact, many of the larger by-products that are similar in structure may also suffer this same fate.

3. *Use the Platinum Ribbon in Addition to the Quartz Tube.* Based on data obtained by pyrolysis on RDX, the ribbon produces different species than the quartz tube. Complementary information may result due to different mechanisms between the two methods. The ribbon may emphasize ring fragmentation as postulated for TNT decomposition. Experiments can be done to differentiate the catalytic effects of the platinum from the longer residence time of by-products in the quartz tube. One possibility is to add platinum powder to the quartz tube in addition to the EM to increase the potential for catalytic pathways.

4. *Analysis of Residues.* This third, generally forgotten fraction of pyrolysis products was briefly studied for only PETN, but the results indicate that interesting compounds are created that can shed light on the breakdown mechanism. Due to reasons listed above, the newly acquired GC/MS/MS with chemical ionization holds much promise as the method of choice for analysis of this residue by direct injection. Perusal of the decomposition products previously observed for TNT also leads to the conclusion that many of these products will be found in the residue fraction.

5. *Alternate Analytical Column.* One of the troublesome areas for data analysis is the co-elution of NO, N_2, CO, and O_2. A search is ongoing to locate and acquire an analytical GC column that can separate these gases to a resolution better than the current PoraPLOT column.

Completion of these types of experiments can advance the understanding of the pyrolytic mechanism and can help establish a database of by-products for each EM. This information will be useful for assessing the potential PIC that may be emitted by an unoptimized incinerator. The hypotheses that pyrolytic by-products are indeed the PIC of concern may be verified by sampling and analyzing the gaseous emissions from an energetic waste incinerator.

A further possibility is the use of pyrolysis to assign a unique signature to each kind or class of EM. For instance, among the three EM studied here, RDX is unique in the production of triazine and formamide. Only TNT produces acetylene and the large number of nitrile-containing compounds without any formation of formaldehyde. PETN is the only EM here with notable methane and ethylene presence in the pyrogram. In this way, components of a mixture of EM can be uncovered merely by a simple pyrolysis experiment without extractions or instrumentation concerns. Another potential use is the determination of contamination levels of EM in building materials. A building that had been used for manufacturing, processing, or storing EM may be inundated with explosives. Pyrolysis of a small amount of the construction material as a first step could provide a measure of the contamination, thereby initiating changes in the demolition procedure.

References

Aron, K., and L.E. Harris, "CARS Probe of RDX Decomposition," *Chem. Phys. Lett.*, vol 103 (1984), p 413.

Bailey, A. and S.G. Murray, *Explosives, Propellants, and Pyrotechnics*, vol II (Brassey's Defense Publishers, London, 1989).

Behrens, R., "Thermal Decomposition of HMX and RDX: Decomposition Processes and Mechanisms Based on STMBMS and TOF Velocity Spectra Measurements," *Chemistry and Physics of Energetic Materials*, S.N. Bulusu, ed., NATO ASI Series, Series C: Mathematics and Physical Sciences, vol 309C (Kluwer Academic Publishers, Dordrecht, Netherlands, 1990), p 347.

Behrens, R., and S. Bulusu, "Thermal Decomposition of Energetic Materials and Temporal Behaviors of the Rates of the Formation of the Gaseous Pyrolysis Products From Condensed-Phase Decomposition of 1,3,5-Trinitrohexahydro-5-Triazine," *J. Phys. Chem.*, vol 96 (1992), p 8877.

Blais, N.C., N.R. Greiner, and W.J. Fernandez, "Detonation Chemistry Studies of Energetic Materials Using Laboratory Scale Samples," *Chemistry and Physics of Energetic Materials*, S.N. Bulusu, ed., NATO ASI Series, Series C: Mathematics and Physical Sciences, vol 309C (Kluwer Academic Publishers, Dordrecht, Netherlands, 1990), p 477.

Botcher, T.R., and C.A. Wight, "Transient Thin Film Laser Pyrolysis of RDX," *J. Phys. Chem.*, vol 97 (1993), p 9149.

Dacons, J.C., H.G. Adolph, and M.J. Kamlet, "Some Novel Observations Concerning the Thermal Decomposition of 2,4,6-Trinitrotoluene," *J. Phys. Chem.*, vol 74 (1970), p 3035.

Dellinger, B., D.L. Hall, J.L. Graham, S.L. Mazer, W.A. Rubey, and M. Malanchuk, *PIC Formation Under Pyrolytic and Starved Air Conditions*, EPA Project Summary, EPA/600/s2-86/006 (July 1986).

Field, J.E., M.M. Chaudhri, K. Mohan, G.M. Swallowe, and W.L. Ng, *Deformation, Fracture and Explosive Properties of Reactive Materials*, DTIC Technical Report (February 1985).

Graham, J.L., D.L. Hall, and B. Dellinger, "Laboratory Investigation of Thermal Degradation of a Mixture of Hazardous Organic Compounds," *Env. Sci. Tech.*, vol 1, No. 20 (1986), p 703.

Hoffsommer, J.C., and D.J. Glover, "Thermal Decomposition of 1,3,5-Trinitro-1,3,5-Triazacyclohexane (RDX): Kinetics of Nitroso Intermediates Formation," *Combust. Flame*, vol 59 (1985), p 303.

Huwei, L., and F. Ruonong, "Investigation of Thermal Decomposition of HMX and RDX by Pyrolysis–Gas Chromatography," *Thermochemica Acta*, vol 138 (1989), p 167.

Johnson, M., *Development of Methodology and Technology for Identifying and Quantifying Emission Products From Open Burning and Open Detonation Thermal Treatment Methods*, DTIC Technical Report, vol 1 (January 1992).

Knight, J.A., and L.W. Elston, *Laboratory Study of Pyrolysis of Explosive Contaminated Waste*, DTIC Tech Report (July 1978).

Menapace, J.A., and J.E. Marlin, "Photochemical Decomposition of Energetic Materials: Observation of Aryl Benzyloxy Nitroxide and Aryl Benzyl Nitroxide Radicals in Solutions of 1,3,5-Trinitrobenzene and Toluene and Their Deuteriated Analogues at 200 K," *J. Phys. Chem.*, vol 94 (1990), p 1906.

National Academy Press, *Prudent Practices for Disposal of Chemicals From Laboratories*, (Washington, DC, 1983), ch 9.

Ng, W.L., J.E. Field, and H.M. Hauser, "Study of the Thermal Decomposition of Pentaerythritol Tetranitrate," *J.C.S. Perkin II* (1975), p 637.

Ostmark, H., H. Bergman, and K. Ekvall, "Laser Pyrolysis of Explosives Combined With Mass Spectral Studies of the Ignition Zone," *J. Anal. Appl. Pyrolysis*, vol 24 (1992), p 163.

Oyumi, Y., and T.B. Brill, "Thermal Decomposition of Energetic Materials 3. A High Rate, In Situ, FTIR Study of the Thermolysis of RDX and HMX With Pressure and Heating Rate as Variables," *Combust. Flame*, vol 62 (1985), p 213.

Oyumi, Y., and T.B. Brill, "Thermal Decomposition of Energetic Materials 12. Infrared Spectral and Rapid Thermolysis Studies of Azide Containing Monomers and Polymers," *Combust. Flame*, vol 65 (1986a), p 127.

Oyumi, Y., and T. Brill, "Thermal Decomposition of Energetic Materials 14: Selective Product Distributions Evidenced in Rapid, Real-Time Thermolysis of Nitrate Esters at Various Pressures," *Combust. Flame*, vol 66 (1986b), p 9.

Rideal, E.K., and A.J.B. Robertson, "The Sensitiveness of Solid High Explosives to Impact," *Proc. Roy. Soc. A*, vol 195 (1948), p 135.

Rogers, R.N., "Combined Pyrolysis and Thin Layer Chromatography," *Anal. Chem.*, vol 39 (1967), p 730.

Roth, J., *The Thermal Decomposition of PETN*, DTIC Technical Report (July 1949).

Schroeder, M.A., "Critical Analysis of Nitramine Decomposition Data: Product Distributions From HMX and RDX Decomposition," *Proceedings of the 18th JANNAF Combustion Meeting*, (Pasadena, CA, October 1981), p 395.

Shackleford, S.A., "Mechanistic Investigations of Condensed-Phase Energetic Material Decomposition Processes Using the Kinetic Deuterium Isotope Effect," *Chemistry and Physics of Energetic Materials*, S.N. Bulusu, ed., NATO ASI Series, Series C: Mathematics and Physical Sciences, vol 309C (Kluwer Academic Publishers, Dordrecht, Netherlands, 1990), p 413.

Snyder, A.P., S.A. Liebman, M.A. Schroeder, and R.A. Fifer, "Characterization of Cyclotrimethylenetrinitramine (RDX) by Pyrolysis H_2O/D_2O Atmospheric–Pressure Chemical Ionization Tandem Mass Spectrometry," *Org. Mass Spectrom.*, vol 25 (1990), p 61.

J.M. Stratta and Associates, Inc. and Life Systems Inc., *Open Burning–Open Detonation Waste Generation Survey and Alternatives Research Study*, Report for the U.S. Army Construction Engineering Research Laboratory (August 1993).

Tirey, D.A., R.C. Striebich, B. Dellinger, and H.E. Bostian, "Comparison of Organic Emissions From Laboratory and Full Scale Thermal Degradation of Sewage Sludge," *Haz. Waste & Haz. Materials*, vol 8 (1991), p 201.

Urbanski, T., *Chemistry and Technology of Explosives*, vol 2 (Pergamon Press, 1964a).

Urbanski, T., *Chemistry and Technology of Explosives*, vol 3 (Pergamon Press, 1964b).

Urbanski, T., *Chemistry and Technology of Explosives*, vol 4 (Pergamon Press, 1964c).

Volk, F., "Analysis of Reaction Products of Propellants and High Explosives," *Chemistry and Physics of Energetic Materials*, S.N. Bulusu, ed., NATO ASI Series, Series C: Mathematics and Physical Sciences, vol 309C (Kluwer Academic Publishers, Dordrecht, Netherlands, 1990), p 511.

Wampler, T., *Applied Pyrolysis Handbook* (Marcel Dekker, Inc., NY, 1995).

Yinon, J., and S. Zitron, *Modern Methods and Applications in Analysis of Explosives* (Wiley, NY, 1993).

Distribution

Chief of Engineers
ATTN: CERD-ZA
ATTN: CERD-M
ATTN: CERD-C
ATTN: CERD-L
ATTN: CEMP
ATTN: CEMP-E
ATTN: CEMP-C
ATTN: CEMP-M
ATTN: CERM 20314
ATTN: DAEN-ZC 20310

Natick RD&E (NARADCOM)
ATTN: DRDNA-F 01760

Army Materials Tech Lab
ATTN: ALCMT-DRK 02172

AMMRC
ATTN: DRXMR-WE 02172

US Army Engineer Divisions
ATTN: Library 02254
ATTN: Tech Info Center

US Army Engineer Districts
ATTN: Library 96205
ATTN: Library 96343
ATTN: Library 99362

US Army Cold Regions Res & Engr Lab
ATTN: Library 03755

Production Base Modernization Activity
ATTN: SMSMC-PBE-C 07806

ARDEC
ATTN: SMCAR-AES-P
ATTN: Technical Library (2)
ATTN: SMCAR-ISE 07806

FORSCOM
ATTN: Facilities Engr 98433

SHAPE
ATTN: Infrastructure Branch Landa 09705

Engineering Societies Library
ATTN: Acquisitions 10017

US Military Academy
ATTN: Department of Geog & Environ Eng 10996

Watervliet Arsenal
ATTN: SMCWV-EH 12189

Red River Army Depot
ATTN: SDSRR-G

Corpus Christi Army Depot
ATTN: SDSCC-ECD Mail Stop 24 78419

Navy Public Works Center
ATTN: Tech Lib CODE 123C

NAVCIVENGRLAB
ATTN: Bldg 560
ATTN: Lib/REs Info Div 93043

Savanna Army Depot
ATTN: SDSLE-VAE

Rock Island Arsenal
ATTN: SMCRI-EH
ATTN: SMCRL-TL
ATTN: Library
ATTN: US Army Indust Engr Activity 61299

US Army Engr School
ATTN: ATSE-DAC-LB
ATTN: ATSE-DAC-LG
ATTN: ATSE-DAC-FL 65473

USAWES
ATTN: CEWES Library 39180

Redstone Arsenal
ATTN: DESMI-KLF

Defense Distribution Region East
ATTN: DDRE-WI 17070

Tobyhanna Army Depot
ATTN: SDSTO-EH 18466

Aberdeen Proving Ground
ATTN: STEAP-DEH 21005

USAEC (2)
ATTN: SFIM-AEC-TSD 21010

USACPW
ATTN: CECPW-E
ATTN: CECPW-FT
ATTN: CECPW-ZC

Engineer Strategic Studies Ctr
ATTN: Library 22060

US Army Belvoir RD&E Ctr
ATTN: Strebe 22060

HQDLA
ATTN: DLA-WI 22304

NAVFACENGCOM
ATTN: DIR R&D Code 03t 22332
Atlantic Division
ATTN: Code 09B 23511

HQ AMC
ATTN: Tech Library 22333

Radford Army Ammunition Plant
ATTN: SMCRA-EN 24141

HQAFCESA/RA
Tyndall AFB 32403

AFESC Program Office
ATTN: British Army Staff 32403

US Army RD&Std Group UK

US Army Harry Diamond Labs
ATTN: SLCHD-SD-TL 20783

US Govt Printing Office 20314
ATTN: Receiving/Depository Section

National Institute of Standards & Tech.
ATTN: Library 20899

Defense Technical Information Ctr
ATTN: DTIC-FAB (2) 22304

67
9/94